Synthesis, Physical and Antimicrobial Studies of Ferrocenyl-*N*-(pyridinylmethylene)anilines and Ferrocenyl-*N*-(pyridinylmethyl)anilines

Eric M. Njogu, Bernard Omondi and Vincent O. Nyamori

School of Chemistry and Physics, University of KwaZulu-Natal, Private Bag X54001, Durban, 4000, South Africa.
E-mail: bjumberic2002@gmail.com / owaga@ukzn.ac.za / nyamori@ukzn.ac.za

ABSTRACT

Ferrocenyl-*N*-(pyridinylmethylene)anilines Schiff bases were synthesized by reaction of 3- or 4-ferrocenylaniline with either 2-, 3-, or 4-pyridinecarboxaldehyde under solvent-free conditions *via* mechanochemistry technique. Products were obtained in excellent yields within 10 min of grinding. The reactions afforded a melt or gummy semi-solid that solidified to the desired Schiff bases within a short time. These Schiff bases were reduced to their corresponding amines, ferrocenyl-*N*-(pyridinylmethyl)anilines, with $NaBH_4$ over neutral Al_2O_3 solid support *via* grinding. Amines were obtained in excellent yields after intermittent grinding for approximately 1 h. Herein, five novel ferrocenyl-*N*-(pyridinylmethylene)anilines (compounds **3**, **4**, **6–8**) and six ferrocenyl-*N*-(pyridinylmethyl)anilines (compounds **9–14**) are reported. Compounds were characterized through FT-IR, ^{1}H-NMR, ^{13}C-NMR, HRMS and SC-XRD techniques. These compounds show visible solvatochromism, when UV-Vis absorption was measured in polar and nonpolar solvents. In changing solvent from polar to non-polar, the Schiff bases exhibited a blue shift while the amines portrayed a red shift. Electrochemical studies on these compounds reveal that redox behaviour of the iron centre is influenced by the position imine or amine groups. Antimicrobial properties of these compounds were studied for *Escherichia coli*, *Staphylococcus aureus*, *Salmonella typhimirium* and *Candida albicans*. Highest activity was recorded against Gram-positive bacteria and fungi.

1. Introduction

Ferrocene (dicyclopentadienyl iron) is a treasured compound discovered serendipitously[1,2] and its structure was determined[3–5] in the early 1950s. This discovery has impacted greatly on the rapid growth of inorganic and bio-organometallic chemistry.[6,7] The unrelenting study on ferrocene and its utilization in many diverse applications are attributed to; (i) the stability of the ferrocene scaffold to moisture, air and temperature; (ii) the ease of functionalizing the cyclopentadienyl rings in ferrocene skeleton *via* electrophilic substitution to give monosubstituted, 1,1'-disubstituted or 1,2-disubstituted moieties rendering it a pertinent building block; (iii) sufficient rigidity of the sandwich structure providing an appropriate chiral environment; (iv) its readily accessible reversible redox couple; (v) stability of the ferrocenyl group in aqueous aerobic media and (vi) its high electron density and aromaticity.[7,8] The ferrocenyl unit is also known to modify the shapes of molecules as well as the physical properties such as colour, polarizability and magnetism.[9] Generally, studies on ferrocene revolve around generation of compounds that are used in materials science,[10] electrochemistry[11,12] catalysis,[13–15] medicinal applications[16–24] and nonlinear optics[25,26] amongst others.

Ferrocene derivatives containing organic fragments bearing one or more heteroatoms such as sulphur,[27] nitrogen,[28] oxygen,[29] and phosphorous[30] have gained prominence. Amongst the *N*-heterocyclic ferrocenyl metalloligands, ferrocenylpyridine metalloligands have been studied for the possibility of exploit-

ing their redox properties in applications such as amperometric sensors for metal ions[31,32] since they facilitate long-range metal–metal interactions in binuclear complexes. The ferrocenylpyridine metalloligands have been employed in coordination of other metals yielding bimetallic systems with excellent anti-cancer potencies comparable to the drug cisplatin, courtesy of the synergistic effect between the two active metals.[21,33,34] Also, ferrocenylpyridine Schiff bases have been found to show broad-spectrum biological activity against pathogenic microbes.[35,36] Complexes of ferrocene-derived Schiff base ligands have shown exceptional high activities towards ring opening of cyclic esters.[37] In addition, liquid crystalline ferrocenyl Schiff bases also known as ferrocenomesogens, show interesting magnetic traits such as paramagnetism and control of the molecular orientation in magnetic fields.[38,39] Moreover, there is high interest in transition metal complexes with electronically communicating metal centres spanned by conjugated systems that make ferrocenyl metalloligands appealing.[31,40,41]

Nonetheless, the chemistry and applications of ferrocenyl ligands with pyridine nitrogen-donors have not been fully developed. Studies on ferrocenylpyridines only began in the recent past and their properties have not been exhaustively described and their optimal potential usage has not hitherto been explored.[42] Furthermore, there are limited precedents, especially when compared to the ferrocenylphosphine ligands where extensive work has been carried out as independently

reviewed by P. Barbaro *et al.*[43] and A. Fihri *et al.*[44] Potential uses of ferrocenylpyridines Schiff bases includes synthesis of materials for usage in electrochemical sensors,[45] homogenous catalysis,[46] cytotoxic agents,[16] antimicrobial compounds,[47–49] antiparasitic,[50] liquid crystals,[51] non-linear optical materials,[52] luminescent systems,[53] as well as coordination of a variety of metal centres to yield novel bimetallic complexes with fascinating architectures,[54,55] organometallic polymers[56] and conducting polymers.[57]

In view of the aforementioned potential applications of ferrocenylpyridines and ferrocene derived Schiff bases, we have prepared a series of novel mono-substituted ferrocenyl-*N*-(pyridinylmethylene)anilines Schiff bases and their corresponding ferrocenyl-*N*-(pyridinylmethyl)anilines secondary amines. These compounds reported herein have great potential in the fields of antimicrobial, nonlinear optics, electrochemistry and coordination chemistry

Though majority of ferrocenyl Schiff base derivatives are synthesized in solution *via* reflux,[58–60] in this study, the compounds were synthesized *via* mechanochemistry (Section 2.2), a relatively faster and greener technique. Reduction of ferrocenyl Schiff bases has previously been reported by use $NaBH_4$ in methanol over a period of long periods;[61,62] however, in this study reduction of the imines was achieved timeously with $NaBH_4$ over a solid neutral Al_2O_3 support *via* mechanochemistry technique as reported in Section 2.3. Electrochemical, thermal and spectroscopic studies of the compounds are reported. The compounds were also investigated for antimicrobial activity against Gram-negative bacteria *Escherichia coli* and *Salmonella typhimirium*; Gram-positive bacterium *Staphylococcus aureus* and the fungal species *Candida albicans*.

2. Experimental

2.1. Materials and Instrumentation

All chemicals were of reagent grade quality purchased from commercial sources and used as received. These included: ferrocene 98 % (Aldrich, USA), sodium borohydride 99 % (Merck, Germany), 4-nitroaniline 98 % (Merck, Germany), 3-nitroaniline 98 % (Fluka, Switzerland), methanol 99.5 % (Aldrich, USA), sodium nitrite 98.5 % (Associated Chemicals Enterprises, South Africa), hexadecytrimethylammonium bromide 99 % (Aldrich, USA), hydrochloric acid 32 % (Merck, Germany), n-hexane 98 % (Glassworld, South Africa), diethyl ether 99.8 % (Aldrich, USA), $CDCl_3$-d_1 99.8 % atom D (Aldrich, USA), 2-pyridinecarboxaldehyde 99 % (Aldrich, USA), 3-pyridinecarboxaldehyde 98 % (Aldrich, USA), 4-pyridine-carboxaldehyde 97 % (Aldrich, USA), methanol 99.5 % (Associated Chemical Enterprise, South Africa), dichloromethane 99 % (Aldrich, USA), *N,N*-dimethylformamide 99.8 % (Aldrich, USA), toluene 99.9 % (Promark Chemicals, South Africa) and chloroform 99 % (Merck, Germany). Nitrogen 5.0, gas technical grade (Airflex Industrial Gases, South Africa), hydrogen gas 5.0 (Air Products, South Africa) Silica gel 60, 0.063–0.2 mm/70–230 mesh (Merck, Germany), aluminium-coated TLC plates, Müeller-Hinton agar (Scharlab) and nutrient broth (Scharlab).

^{1}H- and ^{13}C-NMR spectra were recorded on BRUKER 400 MHz spectrometer (AVANCE[III] 400) in $CDCl_3$. Chemical shift values are reported in ppm and coupling constants in Hz. ^{1}H-NMR spectra were referenced internally using residual protons in the deuterated solvent ($CDCl_3$: $\delta = 7.24$ ppm) and values reported relative to tetramethylsilane ($\delta = 0.00$ ppm). ^{13}C-NMR spectra were similarly referenced internally to the solvent resonance ($CDCl_3$: $\delta = 77.0$) with values reported relative to tetramethylsilane ($\delta = 0.0$ ppm). The infrared spectra were recorded using a

PerkinElmer spectrum 100 FT-IR spectrometer and the data are reported as percentage transmittances at given wavenumbers. High-resolution electro-spray ionization (ESI) mass spectrometry spectra were recorded using a Waters Micromass LCT Premier TOF-MS. Only the molecular ions (M$^+$) and the major fragmentation peaks are reported. The intensities are quoted as percentages of the base peak. UV-Vis spectra were recorded on a PerkinElmer Lambda 35 UV/VIS spectrophotometer in methanol, dichloromethane, toluene, *N,N*-dimethylformamide or chloroform. The emissions on the other hand were recorded on PerkinElmer LS55 Fluorescence spectrometer in methanol, dichloromethane, *N,N*-dimethylformamide or chloroform. All melting points were determined using Stuart Scientific melting point apparatus (SMP10) and co-related with those from the DSC instrument and are uncorrected. DSC thermal analyses were conducted on a SDT Q600 V20.9 Build 20, Universal V4.7A TA Instrument. The samples were heated from room temperature to 600 °C at a rate of 5 °C min^{-1} under nitrogen atmosphere with a gas flow rate of 50 mL min^{-1}. Prior to analysis, the DSC was calibrated with sapphire calibrant while temperature was calibrated using indium and zinc standards. Cyclic voltammograms were performed using a Metrohm 797 VA Computrace electrochemical analyzer with a one compartment three electrode system consisting of Ag/AgCl$_2$ (0.01 M) reference electrode, platinum wire auxiliary electrode and platinum disc working electrode. Samples (*ca.* 0.1 mM) were prepared in acetonitrile and data aquired at a sweep rate of 100 mV s^{-1} under nitrogen atmosphere at ambient temperature. Sodium perchlorate (0.1 M) was used as the background electrolyte. Solutions were saturated with nitrogen by bubbling nitrogen gas for 5 min prior to each run. A standard protocol, the platinum disc working electrode was thoroughly polished between runs. The reference and auxiliary electrodes were also rinsed between runs.

2.2. General Synthesis of Ferrocenyl-*N*-(pyridinyl-methylene)anilines

4-Nitrophenylferrocene and 3-nitrophenylferrocene were synthesized according to reported procedure *via* arylation of ferrocene by diazonium salt under phase transfer conditions.[63] Thereafter, these nitro-derivatives were reduced with molecular H$_2$ gas and 5 % Pd/C in a Parr reactor to obtain 4-ferrocenylaniline (**1**) and 3-ferrocenylaniline (**2**), respectively. Their characterization data are similar to those reported in literature.[21,64]

The ferrocenyl-*N*-(pyridinylmethylene)anilines **3–8** were synthesized by grinding ferrocenylaniline, compound **1** or **2** in combination with apposite pyridinecarboxaldehyde in a pyrex tube fitted with ground joint and a side arm.[65] Grinding for 2–10 min resulted in a paste or in some cases a gummy melt that was dried under reduced pressure to get product as a dry solid. All the physical and spectral data for the known compound, 4-pyridylimine-4′-phenylferrocene (**5**), i.e. colour, m.p, ^{1}H- and ^{13}C-NMR were in line with the ones previously reported.[21] Experimental data for the novel compounds **3**, **4**, and **6–8** are reported in the subsequent subsections 2.2.1 to 2.2.5.

2.2.1. *Synthesis of* (E)-4-ferrocenyl-N-*(pyridinyl-2-methylene)aniline* (**3**)

4-Ferrocenylaniline (**1**) (0.3004 g, 1.08 mmol) and pyridine-2-carboxaldehyde (0.1140 g, 1.06 mmol). The reaction yielded an orange yellow solid that was recrystallized in methanol layered with hexane and this provided orange crystals suitable for X-ray crystallography. Yield 0.3461 g, 89 %, m.p. 138–140 °C, DSC peak m.p. 141.41 °C. $\Delta H_f = 4.55 \times 10^6$ J mol^{-1}. $\Delta S_f = 1.1 \times 10^4$ J mol^{-1} K^{-1}. Calc. for $C_{22}H_{18}N_2Fe$: M$^+$ = 366.0819.

RESEARCH ARTICLE

E.M. Njogu, B. Omondi and V.O. Nyamori,
S. Afr. J. Chem., 2016, **69**, 51–66,
<http://journals.sabinet.co.za/sajchem/>.

53

Found [M$^+$] 366.0825. FT-IR (cm^{-1}): 3084, 1630, 1567, 1521, 1468, 1281, 816, 503 488. ^{1}H-NMR (400 MHz, CDCl$_3$, δ ppm): δ = 8.69 (2H, m, C$_5$H$_4$N), 8.22 (1H, d, J = 7.8 Hz, -CH=N), 7.81 (1H, t, J = 7.5 Hz, C$_5$H$_4$N), 7.51 (2H, d, J = 8.0 C$_6$H$_4$), 7.34 (1H, d, J = 5.4 Hz, C$_5$H$_4$N), 7.27 (2H, m, C$_6$H$_4$), 4.65 (2H, t, J = 1.8 Hz, C$_5$H$_4$), 4.32 (2H, t, J = 1.8 Hz, C$_5$H$_4$), 4.04 (5H, s, C$_5$H$_5$) ppm. ^{13}C-NMR (400 MHz, CDCl$_3$, δ ppm): δ = 152.67 (-CH=N-), 149.70 (C$_5$H$_4$N), 143.44 (C$_6$H$_4$), 136.69 (C$_5$H$_4$N), 136.11 (C$_5$H$_4$N), 129.92 (C$_6$H$_4$), 126.80 (C$_5$H$_4$N), 124.99 (C$_6$H$_4$), 121.82 (C$_5$H$_4$N), 121.44 (C$_6$H$_4$), 84.76 (C$_5$H$_4$), 69.65 (C$_5$H$_4$), 69.39 (C$_5$H$_4$), 69.11 (C$_5$H$_4$), 66.48 (C$_5$H$_5$) ppm.

2.2.2. *Synthesis of (E)-4-ferrocenyl-N-(pyridinyl-3-methylene)aniline* (**4**)

4-Ferrocenylaniline (**1**) (0.3000 g, 1.08 mmol) and pyridine-3-carboxaldehyde (0.1132 g, 1.06 mmol). The product was vacuum dried and gave an orange-yellow solid. Recrystallization in dichloromethane/methanol solution gave orange crystalline plates suitable for X-ray crystallography. Yield 0.3579 g, 92 %, m.p. = 146–148 °C, DSC peak m.p. 146.71 °C, ΔH_f = 6.81 × 10^6 J mol^{-1}, ΔS_f = 1.61 × 10^4 J mol^{-1} K^{-1}. Calc. for C$_{22}$H$_{18}$N$_2$Fe: [M$^+$] = 366.0819. Found [M$^+$] = 366.0818. FT-IR (cm^{-1}): 3089, 2876, 1901, 1623, 1411, 1324, 1281, 821. ^{1}H-NMR (400 MHz, CDCl$_3$, δ ppm): δ = 9.05 (1H, s, C$_5$H$_4$N), 8.72 (1H, s, C$_5$H$_4$N), 8.56 (1H, s, -CH=N), 8.30 (1H, d, J = 7.8 Hz, C$_5$H$_4$N), 7.50 (2H, d, J = 8.4 Hz, C$_6$H$_4$), 7.42 (1H, s, C$_5$H$_4$N), 7.19 (2H, d, J = 8.4 Hz, C$_6$H$_4$), 4.65 (2H, t, J =1.8 Hz, C$_5$H$_4$), 4.32 (2H, t, J = 1.8 Hz, C$_5$H$_4$), 4.40 (5H, s, C$_5$H$_5$) ppm. ^{13}C-NMR (400 MHz, CDCl$_3$, δ ppm): δ = 156.43 (-CH=N), 149.78 (C$_5$H$_4$N), 148.92 (C$_5$H$_4$N), 144.27 (C$_6$H$_4$), 138.21 (C$_5$H$_4$N), 134.77 (C$_6$H$_4$), 126.79 (C$_5$H$_4$N), 122.50 (C$_6$H$_4$), 121.14 (C$_6$H$_4$), 84.71 (C$_5$H$_4$), 69.66 (C$_5$H$_4$), 69.43 (C$_5$H$_4$), 69.12 (C$_5$H$_4$), 66.45 (C$_5$H$_5$) ppm.

2.2.3. *Synthesis of (E)-3-ferrocenyl-N-(pyridinyl-2-methylene)aniline* (**6**)

3-Ferrocenylaniline (**2**) (0.3020 g, 1.09 mmol) and pyridine-2-carboxaldehyde (0.1144 mg, 1.07 mmol). Yield 0.3658 g, 94 %, m.p = 93–94 °C, DSC peak m.p. 93.91 °C, ΔH_f = 6.89 × 10^6 J mol^{-1}, ΔS_f = 1.88 × 10$^{4\,J\,mol^{-1}}$ K^{-1}. Calc. for C$_{22}$H$_{18}$N$_2$Fe: [M$^+$] = 366.0898. Found [M$^+$] = 366.0840. FT-IR (cm^{-1}): 3089, 2876, 1900, 1623, 1411, 1324. ^{1}H-NMR (400 MHz, CDCl$_3$, δ ppm): δ = 8.72 (1H, d, J = 4.3 Hz, C$_5$H$_4$N), 8.66 (1H, s, C$_5$H$_4$N), 8.22 (1H, d, J = 7.9 Hz, C$_5$H$_4$N), 7.82 (1H, td, J = 7.6 Hz, J = 1.4 Hz, C$_5$H$_4$N), 7.39 (3H, m, C$_6$H$_4$), 7.32 (1H, t, J = 7.7 Hz, C$_6$H$_4$), 7.11 (1H, s, -CH=N), 4.67 (2H, t, J = 1.6 Hz, C$_5$H$_4$), 4.32 (2H, t, J = 1.6 Hz C$_5$H$_4$), 4.04 (5H, s, C$_5$H$_5$). ^{13}C-NMR (400 MHz, CDCl$_3$, δ ppm): δ = 160.58 (-CH=N-), 154.60 (C$_5$H$_4$N), 151.08 (C$_6$H$_4$), 149.76 (C$_5$H$_4$N), 140.65 (C$_5$H$_4$N), 136.76 δ = (C$_5$H$_4$N), 129.20 (C$_6$H$_4$), 127.87 (C$_6$H$_4$), 125.20 (C$_6$H$_4$), 124.522 (C$_5$H$_4$N), 122.00 (C$_6$H$_4$), 118.98 (C$_6$H$_4$), 69.46 (C$_5$H$_4$), 69.10 (C$_5$H$_4$), 66.57 (C$_5$H$_5$) ppm.

2.2.4. *Synthesis of (E)-3-ferrocenyl-N-(pyridinyl-3-methylene)aniline* (**7**)

3-Ferrocenylaniline (**2**) (0.3000 g, 1.08 mmol) and pyridine-3-carboxaldehyde (0.1136 g, 1.06 mmol). Yield 0.3650 g, 94 %; m.p. = 95–96 °C, DSC peak m.p 96.16 °C, ΔH_f = 4.3 × 10^6 J mol^{-1}, ΔS_f = 1.15 × 10^4 J mol^{-1} K^{-1}. Calc. for C$_{22}$H$_{18}$N$_2$Fe: [M$^+$] = 366.0819. Found [M$^+$] = 366.0807. FT-IR (cm^{-1}): 3089, 2876, 1900, 1623, 1411, 1324. ^{1}H-NMR (400 MHz, CDCl$_3$, δ ppm): δ = 9.03 (1H, s, C$_5$H$_4$N), 8.70 (1H, s, C$_5$H$_4$N), 8.53 (1H, s, C$_5$H$_4$N), 7.37 (4H, m, C$_6$H$_4$), 7.03 (1H, s, -CH=N), 4.67 (2H, t, J = 1.8, C$_5$H$_4$), 4.32 (2H, t, J = 1.8 Hz, C$_5$H$_4$), 4.05 (5H, C$_5$H$_4$) ppm. ^{13}C-NMR (400 MHz, CDCl$_3$, δ ppm): δ = 157.98 (-CH=N), 151.11 (C$_5$H$_4$N), 150.63 (C$_5$H$_4$N), 142.81 (C$_6$H$_4$), 140.82 (C$_5$H$_4$N), 129.27 (C$_6$H$_4$), 124.80

(C$_5$H$_4$N), 122.32 (C$_6$H$_4$), 119.02 (C$_6$H$_4$), 117.72 (C$_6$H$_4$), 84.56 (C$_5$H$_4$), 69.68 (C$_5$H$_4$), 69.18 (C$_5$H$_4$), 66.60 (C$_5$H$_5$) ppm.

2.2.5. *Synthesis of (E)-3-ferrocenyl-N-(pyridinyl-4-methylene)aniline* (**8**)

3-Ferrocenylaniline (**2**) (0.3017 g, 1.09 mmol) and pyridine-4-carboxaldehyde (0.1141 mg, 1.06 mmol). Yield 0.3721, 95 %: m.p = 125–126 °C, DSC peak m.p 127.68 °C, ΔH_f = 2.7 × 10^6 J mol^{-1}, ΔS_f = 6.77 × 10^3 J mol^{-1} K^{-1}. Calc. for C$_{22}$H$_{18}$N$_2$Fe: [M$^+$] = 366.0819. Found [M$^+$] = 366.0813. FT-IR (cm^{-1}): 3089, 2876, 1900, 1623, 1411, 1324. ^{1}H-NMR (400 MHz, CDCl$_3$, δ ppm): δ = 8.76 (2H, s, C$_5$H$_4$N), 8.47 (1H, s, -CH=N), 7.77 (2H, s, C$_5$H$_4$N), 7.32 (3H, m, C$_6$H$_4$) 7.04 (1H,s, C$_6$H$_4$), 4.67 (2H, t, J = 1.8 Hz, C$_5$H$_4$), 4.32 (2H, t, J = 1.8 Hz, C$_5$H$_4$) 4.04 (C$_5$H$_5$) ppm. ^{13}C-NMR (400 MHz, CDCl$_3$, δ ppm): δ = 157.98 (-CH=N), 151.11 (C$_6$H$_4$), 150.63 (C$_5$H$_4$N), 142.81 (C$_5$H$_4$N), 140.81 (C$_6$H$_4$), 129.27 (C$_6$H$_4$), 124.80 (C$_6$H$_4$), 122.32 (C$_6$H$_4$), 119.02 (C$_6$H$_4$), 117.72 (C$_6$H$_4$N), 69.69 (C$_5$H$_4$), 69.17 (C$_5$H$_4$), 66.60 (C$_5$H$_5$) ppm.

2.3. General Synthesis of the Ferrocenyl-*N*-(pyridinyl-methyl)anilines

The Schiff bases **3**–**8** were reduced to their corresponding secondary amines using NaBH$_4$ over solid neutral Al$_2$O$_3$ support *via* grinding under solvent-free conditions.[66] The NaBH$_4$ and neutral Al$_2$O$_3$ solid-phase mixture was prepared in a porcelain mortar by grinding neutral alumina (2.0 g, 20 mmol) with sodium borohydride (0.34 g, 9.0 mmol) for 5 min. Thereafter, appropriate imine (1.0 mmol) was added followed by addition of five drops of 99 % methanol. The grinding was continued intermittently and the progress of each reaction was monitored by the TLC using dichloromethane. Once all the substrate reacted, (45–60 min), the reaction mixture was poured into 20.0 mL of dichloromethane and filtered through a sintered glass funnel. The residue was washed further with two 15.0 mL portions of the same solvent. The solvent from the filtrate containing the product was evaporated and product purified *via* column chromatography to obtain the secondary amine. All these amine derivatives are new and their experimental characterization data are given in the subsequent subsections 2.3.1 to 2.3.6.

2.3.1. *Synthesis of 4-Ferrocenyl-N-(pyridinyl-2-methyl)aniline* (**9**)

Compound **3**, (0.3662 g, 1 mmol). Recrystallization in methanol gave orange plates suitable for X-ray crystallography. Yield 0.3360 g, 92 %, m.p. = 184–186 °C, DSC peak m.p 184.76 °C, ΔH_f = 3.34 × 10^6 J mol^{-1}, ΔS_f = 7.23 × 10^3 J mol^{-1} K^{-1}. Calc. for C$_{22}$H$_{20}$N$_2$Fe: [M$^+$] = 368.0976. Found [M$^+$] 368.0975. FT-IR (cm^{-1}): 3343, 3082, 2882, 1611, 1594, 1532, 1323, 1293. ^{1}H-NMR (400 MHz, CDCl$_3$, δ ppm): δ = 8.58 (1H, d, J = 3.6 Hz, C$_5$H$_4$N), 7.64 (1H, t, J = 7.5 Hz, C$_5$H$_4$N), 7.34 (1H, d, J = 7.7 Hz, C$_5$H$_4$N), 7.29 (2H, d, J = 8.1 Hz, C$_6$H$_4$), 7.18 (1H, t, J = 5.4 Hz, C$_5$H$_4$N), 6.60 (2H, d, J = 8.1 Hz, C$_6$H$_4$), 4.48 (4H, m, C$_5$H$_4$), 4.20 (2H, s, -CH$_2$-) 4.00 (5H, s, C$_5$H$_5$) ppm. ^{13}C-NMR (400 MHz, CDCl$_3$, δ ppm): δ = 149.89 (C$_5$H$_4$N), 142.5 (C$_6$H$_4$) 136.73 (C$_6$H$_4$N), 127.20 (C$_5$H$_4$N), 122.16 (C$_6$H$_4$N), 121.68 (C$_6$H$_5$), 113.10 (C$_6$H$_4$), 69.36 (C$_5$H$_4$), 68.11 (C$_5$H$_4$), 65.77 (C$_5$H$_5$), 49.43 (-CH$_2$-) ppm.

2.3.2. *Synthesis of 4-Ferrocenyl-N-(pyridinyl-3-methyl)aniline* (**10**)

Compound **4** (0.366 g, 1 mmol). Recrystallization in methanol gave golden yellow plates. Yield 0.3421 g, 93 %, m.p 172–174 °C; DSC peak m.p. 174.70 °C, ΔH_f = 4.572 × 10^6 J mol^{-1}, ΔS_f = 1.02 × 10^4 J mol^{-1} K^{-1} Calc. for C$_{22}$H$_{20}$N$_2$Fe: M$^+$ = 368.0976. Found [M$^+$] = 368.0985. FT-IR (cm^{-1}): 3393, 3260, 3079, 2860, 1611, 1533, 1315, 1293, 1251, 1186. ^{1}H-NMR (400 MHz, CDCl$_3$, δ ppm): δ = 8.67 (1H,

s, C_5H_4N), 8.55 (1H, s, C_5H_4N), 7.70 (1H, d, J = 7.7 C_5H_4N), 7.27 (3H, m, 1H- C_5H_4N, 2H- C_6H_4), 6.56 (2H, d, J = 8.5 Hz, C_6H_4), 4.51 (2H, t, J = 1.8 Hz, C_5H_4), 4.36 (2H, s, -CH_2-), 4.21 (2H, t, J = 1.8, C_5H_4), 4.00 (5H, s, C_5H_5) ppm. ^{13}C-NMR (400 MHz, CDCl$_3$, δ ppm): δ = 149.2 (C_6H_4), 148.75 (C_5H_4N), 145.98 (C_6H_4N), 135.18 (C_5H_4N), 128.55 (C_5H_4N), 127.24 (C_6H_4), 113.05 (C_6H_4), 86.58 (C_5H_4), 69.38 (C_5H_4), 68.21 (C_5H_4), 65.79 (C_5H_5), 46.03 (-CH_2-) ppm.

2.3.3. *Synthesis of 4-Ferrocenyl-N-(pyridinyl-4-methyl)aniline* (**11**)

Compound **5**, (0.366 g, 1 mmol) used. Recrystallization in methanol gave shinny orange plates suitable for X-ray crystallography. Yield 0.3533 g, 96 %, m.p = 189–191 °C, DSC peak m.p 191.31 °C, ΔH_f = 3.84 × 10^6 J mol^{-1}, ΔS_f = 8.28 × 10^3 J mol^{-1} K^{-1}. Calc. for $C_{22}H_{20}N_2Fe$: [M$^+$], 368.0976. Found [M$^+$] 368.0961. FT-IR(cm^{-1}): 3324, 3086, 2917,1603,1535,1417, 1283. ^{1}H-NMR (400 MHz, CDCl$_3$ δ ppm): δ = 8.58 (2H, d, J = 4.0 Hz, C_5H_4N), 7.32 (2H, d, J = 4.0 Hz, C_5H_4N), 7.28 (2H, dd, J = 6.7 Hz, J = 1.8 Hz, C_6H_4), 6.51 (2H, d, J = 8.6 Hz, C_6H_4), 4.50 (2H, t, J = 1.8 Hz, C_5H_4), 4.37 (2H, s, -CH_2-), 4.21 (2H, t, J = 1.8 Hz, C_5H_4) 4.0 (5H, s, C_5H_5). ^{13}C-NMR (400 MHz, CDCl$_3$, δ ppm): δ = 149.97 (C_5H_4N), 147.6 (C_6H_4), 144.63 (C_5H_4N), 139.24 (C_6H_4), 127.25 (C_6H_4), 122.21 (C_5H_4N), 112.97(C_6H_4), 69.37 (C_5H_4),, 68.21(C_5H_4), 65.81(C_5H_5), 47.31 (-CH_2-) ppm.

2.3.4. *Synthesis of 3-Ferrocenyl-N-(pyridinyl-2-methyl)aniline* (**12**)

Compound **6** (0.366 g, 1 mmol) used. Recrystallization in methanol gave orange blocks. Yield; 0.3390 g, 92 %, m.p = 110–112 °C, DSC peak m.p 111.79 °C, ΔH_f = 9.27 × 10^6 J mol^{-1}, ΔS_f = 8.29 × 10^4 J mol^{-1} K^{-1}..Calc. for $C_{22}H_{20}N_2Fe$: [M$^+$] 368.0976. Found [M$^+$]. 368.0984. FT-IR (cm^{-1}): 3362, 3014, 1730, 1603, 1585, 1521, 1434, 1418, 1246, 1144, 1045. ^{1}H-NMR (400 MHz, CDCl$_3$ δ ppm): 8.59 (1H, s, C_5H_4N), 7.63 (1H, d, J = 7.3 Hz, C_5H_4N), 7.36 (1H, d, J = 7.6 Hz, C_5H_4N), 7.17 (1H, d, J = 5.1 Hz, C_6H_4), 7.08 (1H, t, J = 7.7 Hz, C_5H_4N), 6.83 (1H, d, J = 7.3 Hz, C_6H_4), 6.76 (1H, s, C_6H_4), 6.51 (1H, d, J = 7.5 Hz, C_6H_4), 4.55 (2H, t, J = 1.8 Hz, C_5H_4), 4.45 (2H, s, -CH_2-), 4.23 (2H, t, J = 1.8 Hz, C_5H_4), 3.97 (5H, s, C_5H_5) ppm. ^{13}C-NMR (400 MHz, CDCl$_3$, δ ppm): δ = 158.74 (C_5H_4N), 149.02 (C_6H_4), 147.79 (C_5H_4N), 140.12 (C_5H_4N), 136.78 (C_5H_4N), 129.12 (C_6H_4), 122.19 (C_5H_4N), 121.66 (C_6H_4), 116.14 (C_6H_4), 111.16 (C_6H_4), 111.01 (C_6H_4), 86.04 (C_5H_4), 69.56 (C_5H_4), 68.64 (C_5H_4), 66.61 (C_5H_5), 49.42 (-CH_2-) ppm.

2.3.5. *Synthesis of 3-ferrocenyl-N-(pyridinyl-3-methyl)aniline* (**13**)

Compound **7** (0.366 g, 1 mmol) used. Recrystallization in methanol gave deep orange blocks. Yield; 0.3240 g, 88 %, m.p = 88–90 °C. Calc. for $C_{22}H_{20}N_2Fe$: [M$^+$] 368.0976. Found [M$^+$]. 368.0981. FT-IR(cm^{-1}): 3267, 3096, 2920, 1723, 1602, 1536, 1460, 1423, 1309, 1236, 1103, 1024. ^{1}H-NMR (400 MHz, CDCl$_3$ δ ppm): δ = 8.67 (1H, s, C_5H_4N), 8.53 (1H, s, C_5H_4N), 7.72 (1H, d, J = 6.8 Hz, C_5H_4N), 7.28 (1H, s, C_5H_4N), 7.07 (1H, t, J = 7.6 Hz, C_6H_4), 6.85 (1H, d, J = 7.2 Hz, C_6H_4), 6.69 (1H, s, C_6H_4), 6.46 (1H, d, J = 7.4 Hz, C_6H_4), 4.52 (2H, t, J = 1.8 Hz, C_5H_4). 4.39 (2H, s, -CH_2-), 4.24 (2H, t, J = 1.8 Hz, C_5H_4), 3.97 (5H, s, C_5H_5) ppm. ^{13}C-NMR (400 MHz, CDCl$_3$, δ ppm): δ = 149.12 (C_6H_4), 148.68 (C_5H_4N), 147.50 (C_5H_4N), 140.30 (C_5H_4N), 135.16 (C_5H_4N), 129.19 (C_6H_4), 123.10 (C_5H_4N), 120.00 (C_6H_4), 116.55 (C_6H_4), 111.00 (C_6H_4), 85.81 (C_5H_4), 69.60 (C_5H_4), 68.73 (C_5H_4), 66.61 (C_5H_5), 45.95 (-CH_2-) ppm.

2.3.6. *Synthesis of 3-ferrocenyl-N-(pyridinyl-4-methyl)aniline* (**14**)

Compound **8**, (0.366 g, 1 mmol) used. Recrystallization in methanol gave orange blocks suitable. Yield 0.3136 g, 85 %; m.p = 141–143 °C. Calc. for $C_{22}H_{20}N_2Fe$: [M$^+$] 368.0976. Found [M$^+$]. 368.0981. FT-IR(cm^{-1}): 3375, 2919, 2850, 1726, 1586, 1456,

1417, 1246, 1068, 1024. ^{1}H-NMR (400 MHz, CDCl$_3$ δ ppm): δ = 8.75 (1H, s, C_5H_4N), 8.60 (1H, s, C_5H_4N), 7.77 (1H, d, J = 6.0 Hz, C_5H_4N), 7.32 (1H, s, C_6H_5), 7.08 (1H, t, J = 7.5 Hz, C_5H_4N), 6.9 (1H, d, J = 7.6 Hz, C_6H_5), 6.71 (1H, s, C_6H_5), 6.47 (1H, d, J = 7.6 Hz, C_6H_5), 4.53 (2H, t, J = 1.8 Hz, C_5H_4), 4.41 (2H, s, -CH_2-), 4.24 (2H, t, J = 1.8 Hz, C_5H_4), 3.97 (5H, s, C_5H_4) ppm. ^{13}C-NMR (400 MHz, CDCl$_3$, δ ppm): δ = 149.12 (C_5H_4N), 148.68 (C_6H_4), 147.51 (C_5H_4N), 140.30 (C_5H_4N), 135.16 (C_6H_4), 129.19 (C_6H_4), 116.55 (C_6H_4), 111.00 (C_6H_5), 110.8 (C_6H_4), 85.88 (C_5H_4), 69.60 (C_5H_4), 68.73 (C_5H_4), 66.61 (C_5H_5), 45.95 (-CH_2-) ppm.

2.4. Crystal Structure Determination and Refinement

A single crystal of either compound **4**, **9**, **10** and **11** was selected and attached onto the tip of glass fibres using epoxy glue. The crystals were mounted on a Mitegen Micromount and centred in the X-ray beam by using a video camera. The crystal evaluation and data collection were done on a Bruker Smart APEX2 diffractometer with Mo Kα radiation (λ = 0.71073 Å) equipped with an Oxford Cryostream low temperature apparatus operating at 100 K. The initial cell matrix was determined from three series of scans consisting of twelve frames collected at intervals of 0.5 ° in a 6 ° range with the exposure time of ten seconds per frame. Each of the three series of scans was collected at different starting angles and the *APEX*2 program suite was used to index the reflections.[67] The data collection involved using omega scans of 0.5 ° width with an exposure time of 20 seconds per frame. The total number of images was based on results from the program *COSMO,* whereby the expected redundancy was to be 4.0 and completeness of 100 % out to 0.75 Å. Cell parameters were retrieved using *APEX*2 and refined using *SAINT* on all observed reflections. Data reduction was performed using the *SAINT*.[67] software and the scaling and absorption corrections were applied using *SADABS*[68] multi-scan technique. The structures were solved by the direct method using the *SHELXS* program and refined.[68] The visual crystal structure information was performed using *ORTEP*-3 system software.[69] Non-hydrogen atoms were first refined isotropically and then by anisotropic refinement with full-matrix least squares method based on F^2 using *SHELXL*.[68] All hydrogen atoms were positioned geometrically, allowed to ride on their parent atoms and refined isotropically. The crystal data and structural refinement information are summarized in Table 1. All data were subjected to the online checkCIF evaluation criteria.

2.5. Biological Studies

2.5.1. *Inoculation Procedure*

Inoculation of the microorganism used was done in nutrient broth after sterilization. Nutrient broth (1.3 g) was dissolved in distilled water (100 mL). Approximately 10 mL portions of the nutrient broth solution were poured into test tubes. The test tubes were closed with cotton wool plugs which were wrapped with aluminium foil and then sterilized by autoclaving at 121 °C for 15 min. The broth was allowed to cool to 37 °C after which the microorganisms were inoculated. Inoculation was done *via* sterilized cotton swab. The inoculums were incubated at 37 °C for 24 h.

2.5.2. *Preparation of Müller-Hinton Agar Test Plates*

Müller-Hinton agar (38 g) was dissolved in distilled water (1 L). The resulting agar medium was sterilized by autoclaving at 121 °C for 15 min and thereafter allowed to cool in a water bath set at 45 °C. After cooling, approximately 25 mL of the agar medium were poured into previously washed and sterilized

Table 1 Crystallographic and structural refinement data for compounds **4**, **9**, **10** and **11**.

	4	9	10	11
Empirical formula	$C_{22}H_{18}FeN_2$	$C_{22}H_{20}FeN_2$	$C_{22}H_{20}FeN_2$	$C_{22}H_{20}FeN_2$
Formula weight	366.23	368.25	366.23	368.25
Temperature/K	173	173	173	298
λ/Å	0.71073	0.71073	0.71073	0.71073
Crystal system	Monoclinic	Monoclinic	Orthorhombic	Monoclinic
Space group	$P2_1/c$	$P2_1/c$	$Pca2_1$	$P2_1/c$
Unit cell dimensions/Å,°	a = 20.5507(8), α = 90	a = 20.549(7), α = 90	a = 12.262, α = 90	a = 18.584(5), α = 90
	b = 7.5111(3), β = 93.278(2)	b = 10.023(4), β = 94.008(13)	b = 7.683, β = 90	b = 7.734(2), β = 107.099(7)
	c = 10.5766(4), γ = 90	c = 8.220(3), γ = 90	c = 34.538, γ = 90	c = 12.289(3), γ = 90
V/Å³	1629.92(11)	1688.8(11)	3253.8	1688.1(8)
Z	4	4	8	4
σ_{calc}/Mg m⁻³	1.492	1.448	1.495	1.449
Abs. coefficient/mm⁻¹	0.931	0.899	0.933	0.899
F(000)	760	768	1520	768
Crystal size/mm	0.220 × 0.180 × 0.120	0.430 × 0.300 × 0.150	42.000 × 0.280 × 0.140	0.48 × 0.37 × 0.13
θ range	1.985 to 28.715 °	1.987 to 25.500 °	2.359 to 32.683 °	2.29 to 26.00 °
Index ranges	–27 ≤ h ≤26	–24 ≤ h ≤24	–15 ≤ h ≤17	–22 ≤ h ≤22
	–9 ≤ k ≤10	–12 ≤ k ≤12	–10 ≤ k ≤10	–9 ≤ k ≤9
	–13 ≤ l ≤14	–9 ≤ l ≤9	–51 ≤ l ≤52	–15 ≤ l ≤13
Reflections collected	33419	22531	35237	19059
Independent reflections	4114 [R(int) = 0.0220]	3134 [R(int) = 0.0476]	9830 [R(int) = 0.0849]	3321 [R(int) = 0.0578]
Completeness to θ 25.242 °	99.7 %	99.9 %	97.2 %	99.9 %
Data / restraints / parameters	4114 / 0 / 226	3134 / 0 / 226	9830 / 1 / 452	3321 / 0 / 230
Goodness-of-fit on F^2	1.137	1.050	1.130	1.052
Final R indices [I>2sigma(I)]	R1 = 0.0508, wR2 = 0.1340	R1 = 0.0350, wR2 = 0.097	R1 = 0.1008, wR2 = 0.2354	R1 = 0.0318, wR2 = 0.0826
R indices (all data)	R1 = 0.0533 wR2 = 0.1352	R1 = 0.0437 wR2 = 0.1037	R1 = 0.1245 wR2 = 0.2486	R1 = 0.0386 wR2 = 0.0886
Absolute structure parameter	–	–	0.40(6)	–
Largest diff. peak and hole/e.Å⁻³	1.108 and –0.808	0.683 and –0.529	1.116 and –3.077	0.341 and –0.323

Full-matrix least-squares on *F*2 refinement method was applied for all the compounds.

flat-bottomed glass petri dishes to give a uniform depth of approximately 4 mm. The agar medium was allowed to cool to room temperature (*ca*. 25 °C) and set. The test organisms were then struck on the surface of the agar medium using wire loops sterilized by heating red hot in a flame that was then cooled. The paper discs containing the 20 μg of compound under investigation were then loaded onto the already-inoculated agar plates using sterilized forceps and then incubated at 37 °C for 24 h. The diameter of the zone of inhibition was measured around the disc.

A representative sample of each batch of plates without any microorganism was also incubated at the same temperature for 24 h to examine for sterility. Viability of the organisms was tested by incubating test plates without the compounds being investigated. Chloramphenicol was used as the standard antibacterial agent whereas fluconazole was used in the technique as the standard antifungal agent.

3.0. Results and Discussion

3.1. Syntheses

The ferrocenyl-*N*-(pyridinylmethylene)anilines, compounds **3**–**8**, were obtained *via* condensation of 3- or 4-ferrocenylanilines with appropriate pyridinecarboxaldehydes (Schemes 1 and 2). The reactions were carried out by grinding of the reactants under solvent-free conditions in a quartz tube. Progresses of reactions for the formation of Schiff bases were monitored by FT-IR. The obtained melts and in some cases pastes were dried under

vacuum to obtain the final product in excellent yields. All the imines except compound **5**, are new and have not been reported before.

The amine derivatives compounds **9**–**14** synthesized here are all new and have not been reported. These compounds were obtained in excellent yields by solvent-less reduction of corresponding imines *via* the mechanochemistry technique.[66] The imine derivatives were ground on NaBH₄ supported on neutral Al₂O₃ solid-phase and the reaction proceeded *via* the proposed plausible mechanism shown in Fig. 1. The product was extracted by dichloromethane and thereafter purified through column chromatography. Progress of reactions for the formation of the secondary amine derivatives was monitored by FT-IR, as well as TLC on aluminium-coated plates. Synthesis techniques employed here are ecologically benign and also offer considerable synthetic advantages in terms of yield, selectivity, time and simplicity of the reaction procedure.

3.2. Characterization

The synthesized anilines show N-H stretching absorption bands at 3396 and 3217 cm⁻¹ characteristic of the aromatic amines. These N-H stretching bands are absent in the corresponding Schiff bases formed. Hence, the complete disappearance of the N-H stretching band as well as that of the aldehyde C=O stretching band at 1708 to 1699 cm⁻¹ and the corresponding appearance of C=N *sp²* stretching bands ranging from 1623 to 1630 cm⁻¹ confirms the formation of the Schiff bases **3**–**8**. These
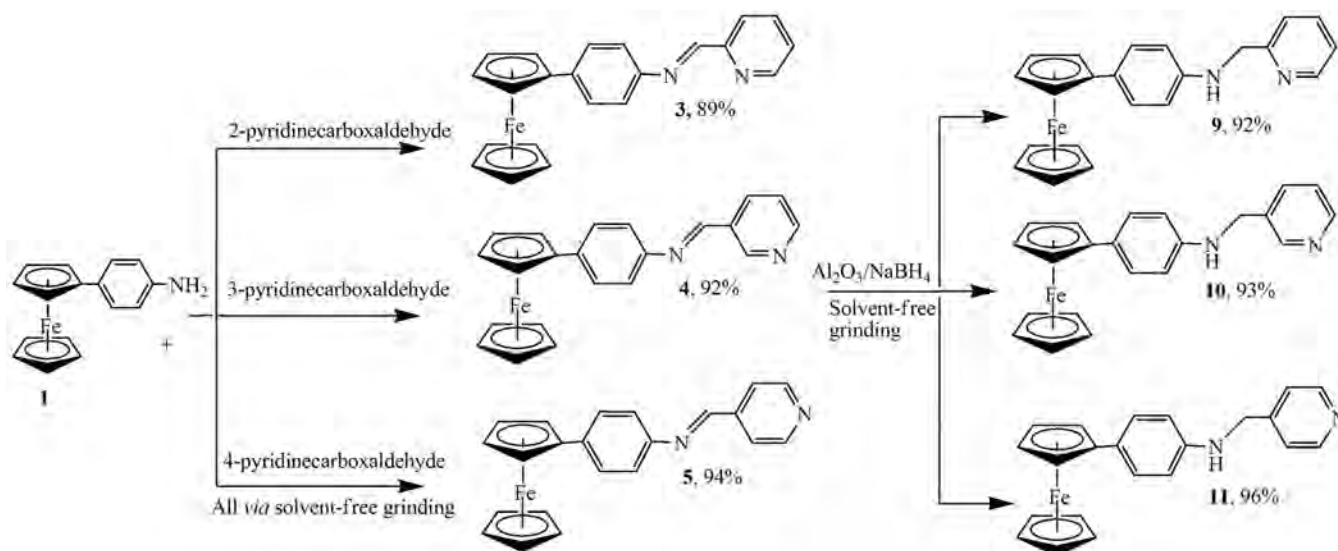
Scheme 1
Solvent-free synthesis route for compounds **3–5** and **9–11**.
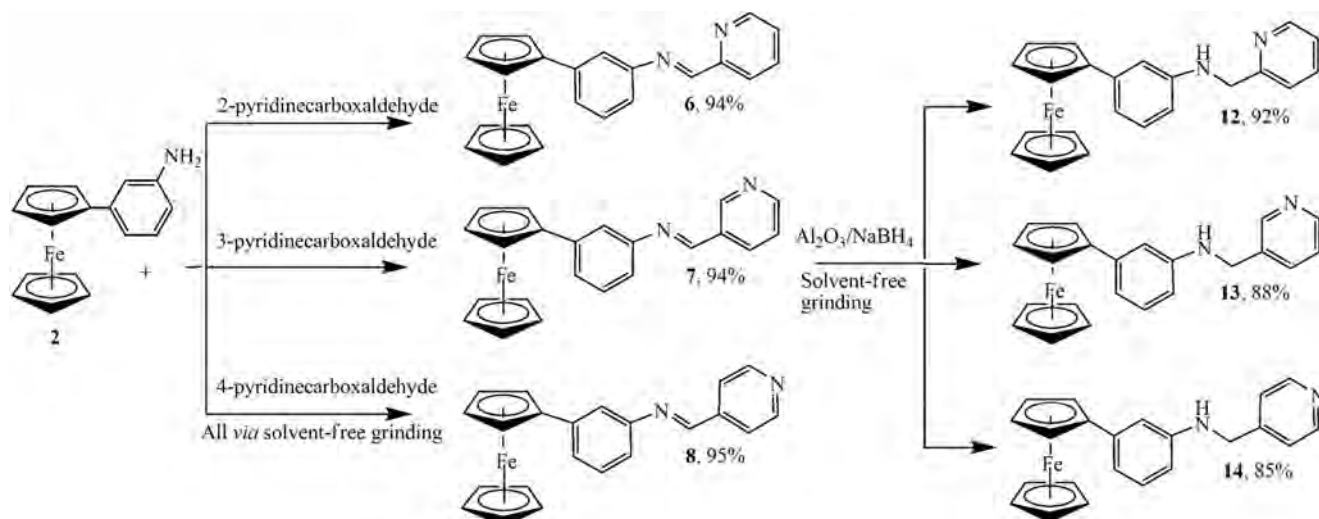
Scheme 2
Solvent-free synthesis route for compounds **6–8** and **12–14**.

characteristic stretching frequencies of the ferrocenyl-*N*-(pyridinylmethylene)anilines Schiff bases are consistent with those reported for similar compounds and theoretical expectations.[21,70,71] Important infrared absorption bands along with their band assignments are listed in Table 2. All the amine derivatives show a medium frequency stretching band between 3260 and 3362 cm⁻¹ assigned to the secondary amine N-H stretch. Moreover, the amine derivatives show stretching frequencies ranging from 1023 to 1188 cm⁻¹ that were assigned to the stretching band of secondary amine C-N sp^3 bond. These secondary amine stretching frequencies are lower than their corresponding C=N sp^2 stretching frequencies. This is expected since the amine bonds are much weaker when compared to the imine bonds and thus the former require lesser energy to stretch. The amines also show a stretching band ranging between 3000 and 2840 cm⁻¹, characteristic to C-H stretch of the sp^3 methylene group. These compounds show characteristic absorption peaks for Fe-Cp stretching vibrations ranging from 479 to 490 cm⁻¹. These infrared stretching bands are not unusual and have been observed in other ferrocenyl Schiff bases.[9] The condensation reaction leading to formation of the Schiff bases and the structural assignments were further supported by the ¹H-NMR spectra for compounds **3–8** where the imine N=CH- proton peak appears in the aromatic region. These peaks corresponds to up-field shift of the aldehyde peak of the pyridinecarboxaldehydes from 10.5 ppm, to 7.2–8.5 ppm in the imines.

For instance, in the ¹H-NMR for compound **4**, the imine proton resonates at 8.56 ppm. The protons of the pyridine ring appear at 9.05, 8.72, 8.56, 8.30 and 7.42 ppm. The two sets of proton in the phenyl ring appear at 7.50 and 7.19 ppm with their coupling constant being 8.4 Hz. The two sets of protons in the substituted cyclopentadienyl ring appear at 4.65 and 4.32 ppm while the five protons in the unsubstituted ring appear at 4.40 ppm. The ¹³C-NMR spectra of these compounds show the imine carbon is the most deshielded and it is registered between 150 to 160 ppm. For instance, the ¹³C-NMR spectrum of compound **4** shows a peak associated with the most deshielded carbon at 156.43 ppm and this peak is accordingly assigned to the imine carbon. The aromatic carbons appear in the region from 121–149.78 ppm and those of the cyclopentadienyl at 66.65–84.71 ppm. These distributions of protons and carbon peaks is in tandem with the proposed structure and confirms the formation of the target
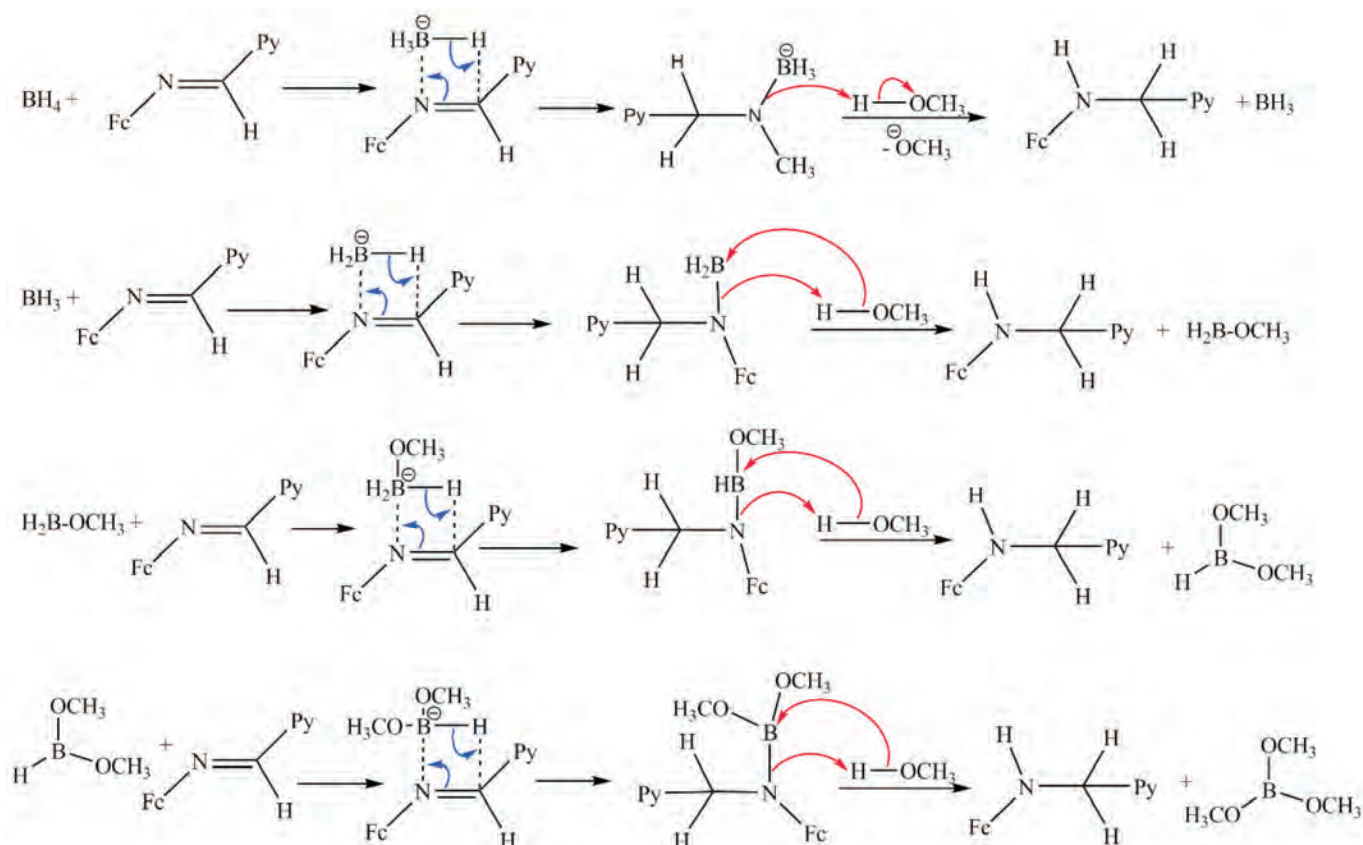
Figure 1 Proposed plausible mechanism for reduction of the imines **3**–**8** with $NaBH_4$ activated on Al_2O_3 solid-phase.

compound. The other imines reported here show similar trends in both the proton and carbon spectra as indicated in the experimental section for each of them (see Supplementary material). These NMR data are consistent with the reported data of similar compounds.[21,71]

Upon reduction of imines **3**–**8** to their corresponding amines **9**–**14**, major upfield shifts in peaks for almost all the protons are observed. Upon conversion of the imine to amine, the proton peaks for the sp^2 methine group, =CH–, are shifted upfield to *ca* 4.4 ppm, characteristic to sp^3 methylene group –CH_2–. In compound **10** for instance, these proton are now observed at 4.36 ppm and their peak integrates to two protons. The protons on the alpha carbon atoms of phenyl ring (with respect the amino group) now resonate at 6.56 ppm down from 7.50 ppm. The alpha protons of the pyridine ring (with respect to the substitution and N atom) resonate at 8.67 ppm in compound **10**, down from 9.05 ppm in compound **4**. All the other amines show similar trends in shift of proton peaks. There is also an upfield

shift of the imine carbon peaks to 46.03 ppm in compound **10** from 156.43 ppm in compound **4**. This is in agreement with the conversion of the carbon from the sp^2 to sp^3 after reduction. Similarly, the amine carbon peaks in the other ferrocenyl-*N*-(pyridinylmethyl)anilines **9**, **11**–**15** appear between 45–50 ppm. As expected, these carbon atoms exhibit negative peaks in the DEPT ^{13}C-NMR in the same position (ppm). The ESI mass spectrum of each of these compounds showed a molecular ion peak (100 %) that corresponds to the mass parent molecule. No major fragmentations were recorded. These data correlate well with that reported in literature for ferrocenyl compounds having secondary amine functional groups.[29] The absolute structures of some of these compounds were confirmed by X-ray crystallography technique as discussed in Section 3.3.

3.3. X-ray Crystallography of Compounds 4 and 9–11
Single crystals for X-ray analysis for compound **4** were grown in dichloromethane/methanol while those of compounds **9**, **10**

Table 2 IR spectral data (selected stretching frequencies).

Compound	ν(C-H) methylene	ν(C-H) methine	ν(C-N) Ph-N	ν(C=N) imine	ν(C-N) amine	ν(N-H)
3	–	3084	1281	1630	–	–
4	–	3090	1280	1629	–	–
6	–	3089	1283	1623	–	–
7	–	3089	1251	1623	–	–
8	–	3089	1286	1623	–	–
9	3082	–	1248	–	1186	3343
10	2860	–	1251	–	1186	3260
11	3027	–	1270	–	1188	3325
12	3014	–	1246	–	1023	3362
13	3096	–	1236	–	1024	3267
14	2919	–	1246	–	1023	3326

and **11** were obtained from methanol, all as orange plates. The asymmetric unit for compound **10** contains two independent molecules related by an inversion centre, similar to that reported in the crystal structure of compound **5**.[21] On the other hand, the asymmetric units in compounds **4**, **9** and **11** each contain a single molecule. The two molecules in the structure of compound **10** have different conformations. Each of these compounds bears a ferrocenyl imine moiety (from the starting ferrocenyl aniline) and a methyl pyridinyl moiety from the starting pyridine carboxaldehyde forming the (*E*)-4-ferrocenyl-*N*-(pyridinyl-3-methylene)aniline Schiff base **4**, and ferrocenyl-*N*-(pyridinylmethyl)anilines, compounds **9–11** on reduction of the respective Schiff bases. Figure 2 shows *ORTEP* diagrams for four compounds.

The two moieties referred in Fig. 2 seem to be the two main sets of planes that describe the conformations in some of the four compounds discussed here. The dihedral angles between these two planes seem to differ from compound to compound and in compound **10**, between the two molecules in the crystal structure. In the structure of compound **10** the dihedral angle between the two molecules 89.011(0.082) ° in one and 84.129(0.089) ° in the second. The difference in the conformations of the two molecules is further depicted in the molecule overlay diagram in Fig. 3. The root mean square deviation of one from the other molecule is 0.0748 Å. In the overlay it is also evident that the methyl pyridinyl moiety is twisted by about 180 ° in the second molecule.

The conformation in compound **4** seems to be different from those of compounds **9–11**. In **4** the substituted cyclopentadienyl ring and the phenyl imine moiety are not coplanar and have a dihedral angle of 15.69(0.175) °. The phenyl imine moiety is also twisted from the plane of the methyl pyridinyl moiety through a dihedral angle of 49.18(07) ° very similar to those reported in literature for similar compounds.[72,73] The conformations of the molecules in the structures of compounds **9** and **11** seem to have two major planes similar to those of the two molecules in compound **10**. However, in the molecular structures of the two compounds the dihedral angle between the ferrocenyl phenyl amine moiety and a methyl pyridinyl moiety is 72.097(0.048) and 83.059(0.055) ° in **9** and **11**, respectively. The observed disparities in orientation of the various moieties in the Schiff base **4** compared to the ferrocenyl-*N*-(pyridinylmethyl)anilines, compounds **9–11** can be attributed to the presence of imine group in **4** that is adequate in providing pi orbitals to maintain conjugation within the entire molecule.[71] This conjugation is, however, broken upon reduction of the imine to secondary amines in compounds **9–11**. This behaviour of secondary amines bearing a ferrocenyl moiety is not exceptional and has been previously documented.[38]

Fundamental bond lengths, angles, planes and interactions are presented on Table 3. The C-N$_{imine}$ and N$_{imine}$-C$_{Ph}$ bond distances in **4** are significantly different from those in **9–11** as expected. In compound **4**, the C—N$_{imine}$ bond distance is 1.276(5) Å while the N$_{imine}$-C$_{Ph}$ is 1.422(4). The corresponding bond distances, i.e.

(a)

(b)

(c)

(d)
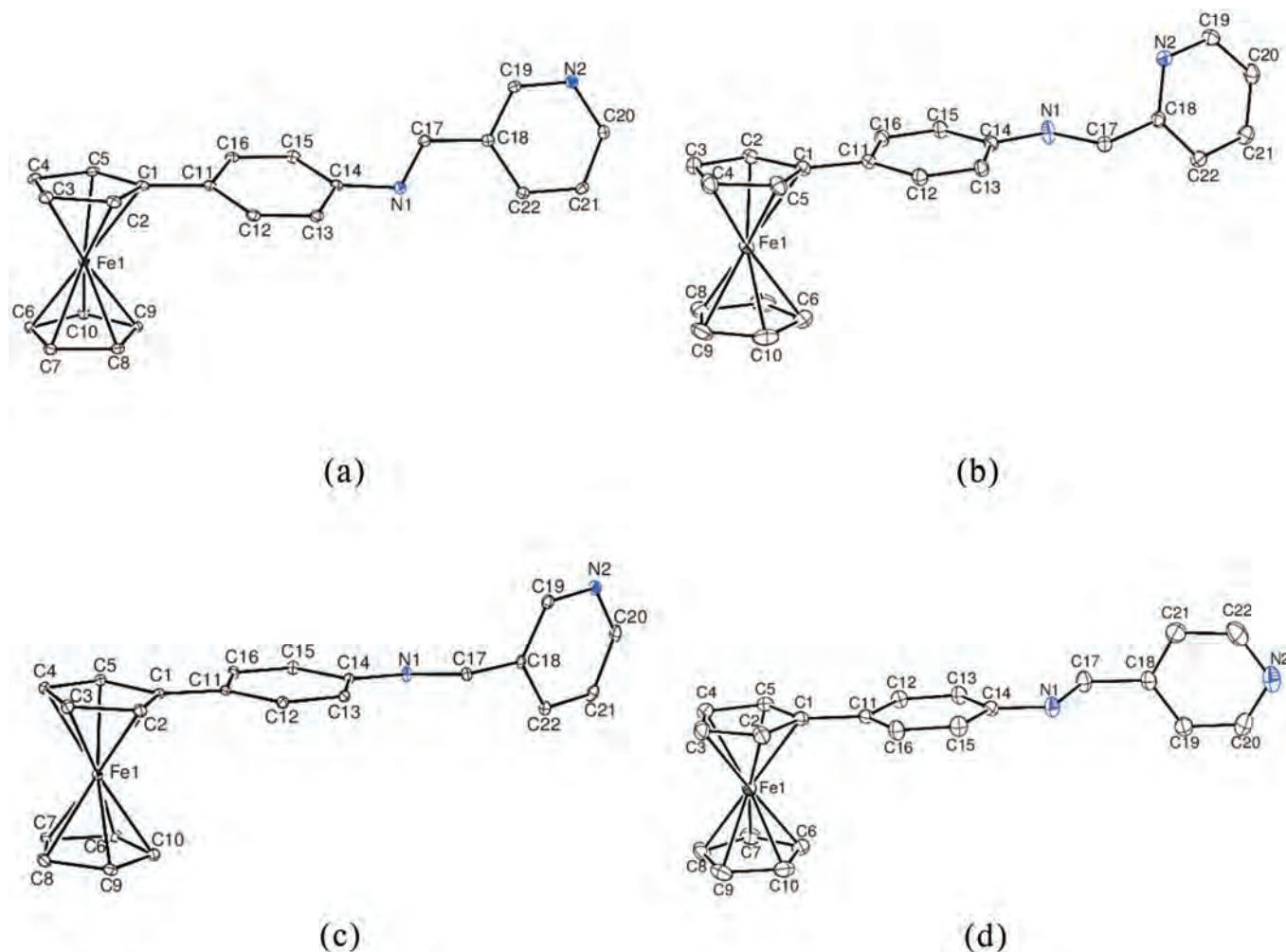
Figure 2 *ORTEP* drawings for compounds **4** (**a**), **9** (**b**), **10** (**c**), and **11** (**d**), showing the atom numbering scheme and thermal motion ellipsoids (50 % probability level). Only one of the two molecules in compound **10** is shown here and for all compounds hydrogen atoms have been omitted for clarity.

Table 3 Selected bond lengths (Å), bond angles (°) and planes for compounds **4**, **9**, **10** and **11**.

Compound:	4	9	10		11
Bond length					
Ph-N$_{imine/amine}$	1.422(4)	1.381(2)	1.388(2) 1.374(2)		1.387(2)
C$_{methine/methylene}$-N$_{imine/amine}$	1.272(5)	1.445(2) 1.465(2)	1.445(2)		1.443(3)
Bond angles					
C$_{Ph}$-N$_{imine}$-C$_{methylene}$	118.57(3)	121.90(1)	119.70(1) 119.52(1)		120.49(2)
N$_{imine}$-C$_{methylene}$-C$_{py}$	122.08(3)	111.04(1)	111.29(1) 111.25(1)		110.61(2)
Planes					
[Cp$_{(subs)}$]-[PhN]	15.69(0.175)	7.114(0.117)	2.356(0.237) 1.481(0.235)		2.96(1)
[PhN]-[CPy]	49.18(0.072)	72.097(0.048)	89.011(0.082) 84.129(0.089)		83.059(0.055)
[Cp$_{(subs)}$PhN]-[(CPy)]	–	–	84.66(3) 88.95(2)		–
Cp$_{(subs.)}$–Cp$_{(unsubs.)}$ torsion angles			1	2	
C1-C6	7.76	12.97	23.77	20.97	21.48
C2-C7	7.98	13.37	24.22	22.22	21.66
C3-C8	7.47	13.27	23.78	21.28	21.03
C4-C9	7.39	12.67	23.20	20.78	21.47
C5-C10	7.21	13.00	23.29	21.09	21.97
Average	7.56	13.06	23.75	21.27	21.52
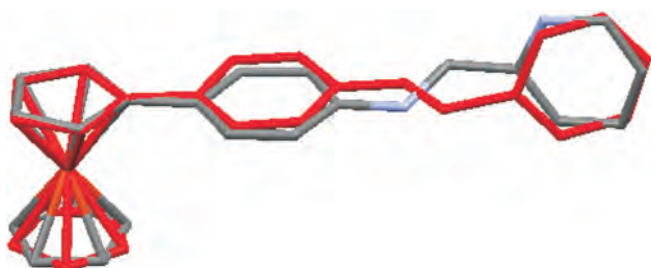
Figure 3 An overlay of the two molecules in the asymmetric unit of compound **10**. Hydrogen atoms omitted for clarity.

C-N$_{amine}$ and N$_{amine}$-C$_{Ph}$ in **9**–**11** are much longer than those in compound **4**. The C-N$_{amine}$ distances are 1.445(2) and 1.465(2) Å for the two molecules in **10**, 1.445(2) and 1.443(3) Å in **9** and **11**, respectively. The Na$_{mine}$-C$_{Ph}$ distances are 1.388(2) and 1.374(2) Å in **10**, 1.381(2) and 1.387(2) for compounds **9** and **11**. Compounds **6** has an imine bond which has greater electron density in the inter-nuclei region that contribute to a stronger bond which is shorter whereas compounds **9**–**11** have single amino bond which relatively weaker and thus longer.

Table 4 lists important intermolecular interactions in compounds **4**, **9**, **10** and **11**. The compounds also show non classical interactions yielding supramolecular structures. Compound **4** for instance shows significant intermolecular π–π interactions involving the pyridinyl and phenyl rings. Consequently, this orients the molecule in a manner leading to formation of C—H…N and π…π intermolecular interactions forming chains in which molecules are stacked in an alternating head-to-tail manner down *b* crystallographic axis. Compound **9** has N—H…N interactions down the *c* crystallographic axis: This interaction leads to the formation of a step-like supramolecular structure.

Compounds **9** and **11** show reasonable intermolecular hydro-

Table 4 Hydrogen bonding parameters and intermolecular interactions for compounds **4**, **9**, **10** and **11**.

Compound:	4	9	10	11
Lengths	2.66(3)	2.54(2)	2.14(1)	2.37(2)
Angles/H-D…A)	160	161	167	166
π–π **interactions**				
Lengths/Å				
Py-Ph	3.929	–	3.532	3.797
C-H35-$\pi_{cp\text{-}subs}$	–	–	2.868	–
C-H39-$\pi_{cp\text{-}subs}$	–	–	2.993	–
Angles /°				
C-H35-$\pi_{cp\text{-}subs}$	–	–	156	–
C-H39-$\pi_{cp\text{-}subs}$	–	–	172	–

gen bonding with bond distances of 2.54(3) and 2.37(2) Å, respectively. The donor atoms are pyridinyl nitrogen atoms in both cases. This results in a step-like supramolecular structure in compound **9** and dimer in compound **11**. The hydrogen bonding and stability of the dimer in compound **11** are further buttressed by intermolecular π–π interactions involving the pyridinyl rings. Compound **10**, shows intermolecular π–π interactions between the pyridinyl and phenyl rings and C-H…π interactions involving the substituted Cp ring in one of the molecules.

3.4. Thermal Studies

Despite having both the phenyl and pyridinyl moieties, in addition to the ferrocenyl group, the compounds reported have sharp melting points similar to ferrocenyl derivatives having only a single phenyl unit[74] Ferrocenyl compounds having one longer axis where two phenyl units are linked to one Cp ring in series forming a chain generally show crystal-crystal phase

transitions while those with three or more phenyl usually show liquid crystalline properties and crystal phase transitions.[10,29,38,74] Compounds reported here lack these credentials (i.e. long linear shape and large length-depth ratio) to generate intermolecular interactions leading to mesomorphism. Therefore, the DSC data for compounds reported show a single key event, i.e. melting and subsequent decomposition. The data obtained for the compounds are listed in Table 5. The molecules for the imine deriva-

Table 5 Physical and analytical data.

Compound	Yield /%	HRMS (ESI-TOF) m/z: [M]$^+$		Melting point/°C
		Calc.	Found	
3	89	366.0819	366.0825	138–140
4	92	366.0819	366.0818	146–148
5	94	366.0898	366.0840	93–94
6	94	366.0819	366.0807	95–96
8	94	366.0819	366.0831	125–126
9	91	368.0976	368.0975	184–186
10	93	368.0976	368.0985	172–174
11	96.	368.0976	368.0961	189–191
12	92	368.0976	368.0984	110–112
13	88	368.0976	368.0981	88–90
14	85	368.0976	368.0981	141–143

tives from 3-ferrocenylaniline have lower melting points compared to those derived from the 4-ferrocenylaniline. Among, the imine derivatives from 3-ferrocenylaniline the melting points increase in the order compound **6** < **7** < **8**. From these studies, it is also evident that the amine derivatives have higher melting points than their corresponding imines from which they were obtained. Therefore, the amines exhibit stronger intermolecular forces that might also be reinforced by hydrogen bonding like in compound **9**. The position of the pyridine nitrogen and also the position of substitution on the phenyl ring (i.e. 3- or 4-ferrocenylaniline) influence the thermal properties of the compounds.

3.5. Photophysical Studies
The UV/Vis absorption and emission of the compounds were carried out in solution at room temperature.

3.5.1. *Solvatochromism Studies*
The metalloligands reported are soluble in a variety of organic solvents and this allowed detailed investigation of their solvatochromic behaviour. The solvatochromism characteristics were studied by measuring the UV-Vis spectra of compounds **3**, **4** and **6–14** in polar (methanol, *N,N*-dimethylformamide), mid-polar (acetonitrile and chloroform), and nonpolar (toluene) solvents. As anticipated, in all solvents, all the compounds showed a bathochromic (red) shift in comparison to pristine ferrocene. The imines and amines displayed both n–π^* and π–π^* transitions[60,75] in methanol. The stronger and higher energy peak were attributed to the π–π^* transition of the Schiff base chromophores and the benzene ring while the weaker and less energetic peaks were assigned to the n–$\pi^{*[60]}$ transition involving the promotion of the lone pair electron of imine nitrogen atom to the antibonding π orbital associated with the Schiff base group. Weaker bands appearing at longer wavelengths can be attributed to the d–d transitions. On changing solvent from nonpolar to polar, all the imines showed a bathochromic shift of π–π^* transitions[75] an indication of their non-linear optics character, a behaviour that has also been observed in other ferrocenyl imine derivatives.[52,75,] These spectral characteristics of the ferrocenyl-*N*

-(pyridinylmethyl)anilines are attributed to the mixing of appreciable metal-to-ligand charge transfer (MLCT) character into their low-energy electronic excited states.[76] This MLCT contribution originate from vectorial displacement of electron density from the metal to the ligand. Conjugation between the π orbitals of the cyclopentadienyl, phenyl and pyridyl rings allows the transferred charge to be delocalized over several atoms, consequently stabilizing the MLCT excited state relative to the ground state and lowering the transition energy. Also, the polar solvents lower the transition energy owing to the greater Coulombic stabilization of the dipolar (charge-separated) excited state. Increase in the intensity of the absorption bands is as a result of mixing charge transfer character into the transition thus reducing the Laporte forbidden character.[76] The observed shifts of band maxima to higher energies in polar solvents point to presence of a polar ground state and nonpolar excited state in imines, i.e. compounds **3**, **4** and **6–8**.

On the other hand, the amine compounds **9–14** showed hypsochromic shift[77] when in polar solvent (methanol) compared to the non-polar (toluene), an indication of possible hydrogen-bonding between the compounds and polar solvent molecules. These compounds have a dipole involving the amino N atom and its H atom. The polar solvent increases the contribution of the polar unit of the molecule in the ground state. Upon transition, the dipole associated with the molecule is either reversed or rotated, subsequently this alteration leads to a hypsochromic shift (negative solvatochromism).[77,78] The hypsochromic shift is consistent with diminished conjugation in the amine. The amines absorb at longer wavelengths when compared to their corresponding imines and this is due to change in the hybridization of N atom upon reduction. The solvatochromic behaviour of these compounds is well in line with the nonlinear optical properties (Table 6) and warrants further investigation and application. The absorption spectra of the compounds in methanol and toluene are shown in Fig. 4. The absorption

Table 6 Maximum absorptions (λ_{max})/nm of the compounds in various solvents.

Compd	Solvent				
	Methanol	DMF	Chloroform	Acetonitrile	Toluene
3	289	288	286	286	284
	252	343	242, 346	242, 340	347
4	286	287	285	284	285
	245, 330	344	245, 346	242, 340	347
6	289	284	283	283	284
	–	–	242	242	
7	289	283	280	286	284
	252	–	243	340	
8	291	281	277	279	285
	–	–	241	235	
9	294	299	296	295	298
	257	226, 446	258	258	–
10	292	299	295	295	297
	256	–	257	257	–
11	294	298	294	294	296
	256	–	256	256	–
12	231	268	243	231	284
	316	321	314	317	317
13	231	268	243	231	286
	316	317	315	317	317
14	231	267	243	231	286
	316	319	314	317	317

RESEARCH ARTICLE

E.M. Njogu, B. Omondi and V.O. Nyamori,
S. Afr. J. Chem., 2016, **69**, 51–66,
<http://journals.sabinet.co.za/sajchem/>.

61
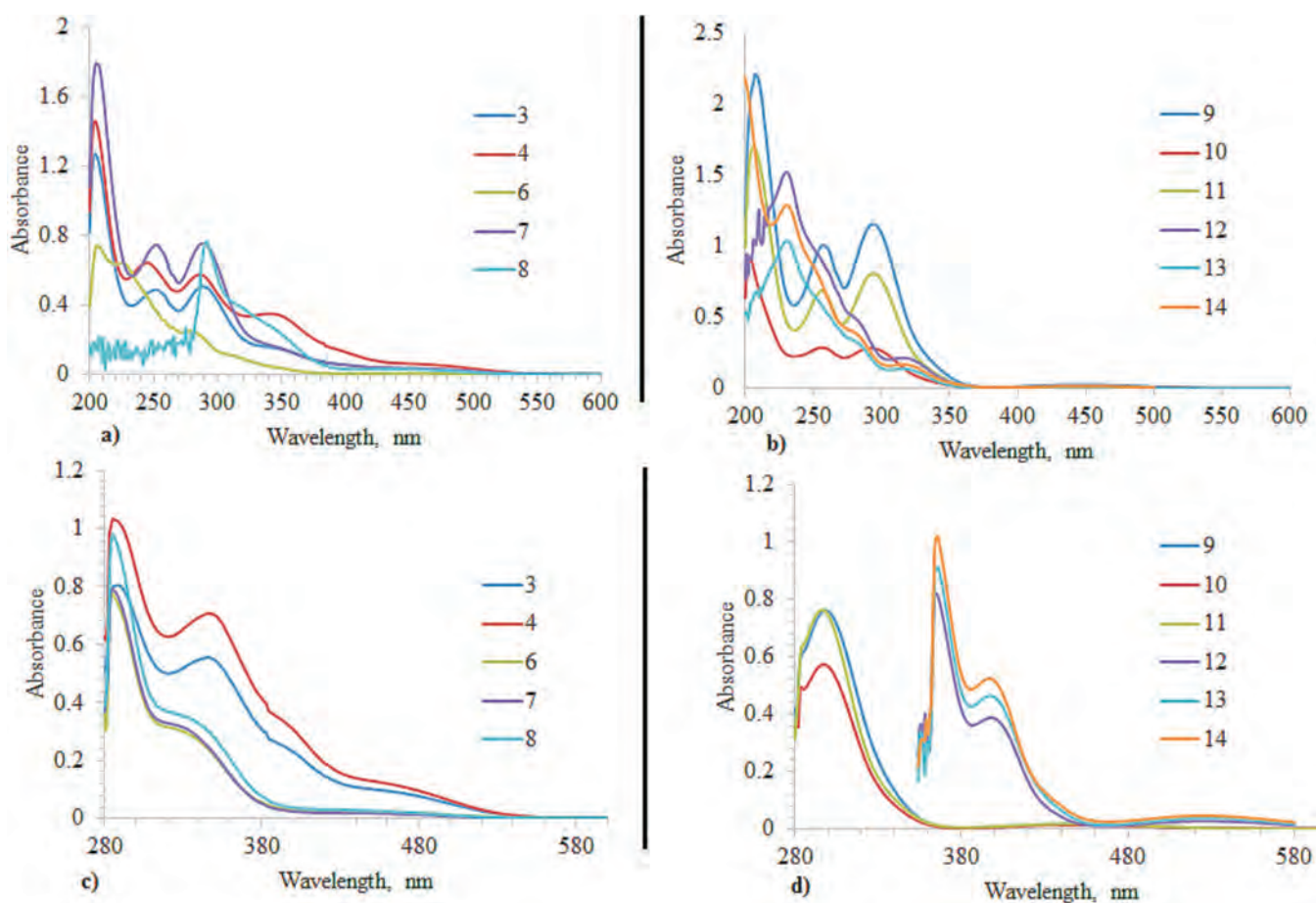
Figure 4 UV-Vis spectra; (**a**) compounds **3–8** in methanol; (**b**) compounds **9–14** in methanol; (**c**) compounds **2–8** in toluene; (**d**) compounds **9–14** in toluene.

maxima of these compounds in solvents with different polarities are summarized in Table 6.

3.5.2. *Fluorescent Spectral Studies*

The emissions of the compounds **3**, **4** and **6–14** were determined in various solvents at room temperature (298 K) and the maximum emissions are reported in Table 7. Ordinarily, aromatic ligands/heterocyclic compounds are not strongly emissive at room temperature.[76] In addition, ferrocene does not show luminescence, because in its excited states, it undergoes very rapid electronic and vibrational relaxation to the ground state.[76] However, in solution at room temperature, all the compounds studied here show broad emission bands, with large stoke shifts averaging between 28–30 nm. This is indicative of molecular fluorescence with short-lived excited states as deduced from the stable emissions.[53] The stable emissions can be allied to the presence of a phenyl ring in the compounds which helps to obliterate nonradioactive decay of the intra-ligand π–π^* transition. The emissions in the compounds stem from the π–π^* transition emissions on the ferrocenyl moiety as well as the phenyl units.[79] The results highlight the applicability of these compounds as fluorophores in detection and determination of absorbing species. The emission spectra of the compounds in methanol are shown in Fig. 5, while the emission maxima in various solvents are summarized in Table 7.

3.6. Electrochemical Studies

Ferrocene is an ideal compound to study electrochemically due to its easily accessible and reversible one-electron redox couple, i.e. Fe^{2+}/Fe^{3+}. Substitutions on the cyclopentadienyl ring

with groups bearing electron withdrawing groups substantially influences the electron density and redox properties of the ferrocenyl iron centre.[73] In view of these, the electrochemical properties of the compounds **3**, **4** and compounds **6–14** were studied by cyclic voltammetry. This was performed in acetonitrile, 2.0×10^{-4} M concentration using 0.1 M sodium perchlorate supporting electrolyte at 100 mVs^{-1} scan rate within a potential range of –1.00 to 1.00 V using Ag/Ag$^+$ as the reference electrode (see section 2.1). All solutions were purged with nitrogen gas prior to experiment and the nitrogen cloud was maintained on the surface of the solution during analysis. The cyclic voltammograms of the Schiff bases and the amines are shown in Fig. 6 where each voltammogram shows one reversible process with one cathodic wave and one anodic wave. This is attributable to the one electron reversible Fe^{2+}/Fe^{3+} redox system of the ferrocenyl moiety. The data obtained from the cyclic voltammograms of the compounds **3**, **4** and **6–14** are different from those of ferrocene and are summarized in Table 8. The peak potential values range from +0.2916 to +0.4642 V for the anodic waves and from +0.3670 to +0.4820 V for the cathodic wave. From these results, the separation of the anodic and the cathodic peak potentials, ΔE_p values are the same for compounds **3**, **7** and **8**, but slightly different formal potentials, E°, as tabulated in Table 8. Compounds **9** and **10** have similar ΔE_p values too, with a small positive shift (0.1071 V), in the formal potential E° observed in compound **10** compared to compound **9**. The imines have higher redox potentials than the amines, suggesting the efficiency of delocalization and electron withdrawing ability of the pyridine moiety.[73] These discrepancies corresponds with decrease on the influence of the pyridinyl ring on the ferrocenyl moiety a

RESEARCH ARTICLE

E.M. Njogu, B. Omondi and V.O. Nyamori,
S. Afr. J. Chem., 2016, **69**, 51–66,
<http://journals.sabinet.co.za/sajchem/>.

62

Table 7 Emission spectra of compounds **3**, **4** and **6–14** in varying solvents.

Compound	Solvent Methanol(λ_{Exc}) λ_{Em}/nm	DMF (λ_{Exc}) λ_{Em}/nm	Chloroform (λ_{Exc}) λ_{Em}/nm	Acetonitrile (λ_{Exc})λ_{Em}/nm
3	(289), 317	(288), 317	(286), 317	(286), 318
4	(286), 316	(287), 316	(285), 315	(284), 312
5	(289), 317	(284), 313	(283), 312	(283), 312
6	(289), 317	(283), 312	(280), 309	(286), 315
8	(291), 320	(281), 309	(277), 305	(279), 307
9	(294), 325	(299), 332	(296), 327	(295), 325
10	(292), 322	(299), 330	(295), 327	(295), 323
11	(294), 323	(298), 314	(294), 324	(294), 324
12	–	(267) 283	–	–
13	–	(267) 2933	–	–
14	–	(267) 282	–	–

Key: λ_{Exc} = excitation wavelength, λ_{Em} = maximum emission wavelength.

consequence of the broken conjugation. Compound **8** has the highest $E°$ and thus higher tendency reduction. Compound **9** on the other hand has the lowest $E°$ and thus is the least favourable in facilitating the reduction of the iron centre. These data show that the position of pyridine nitrogen as well as ferrocene on the phenyl ring, affects electron transfer process and consequently redox behaviour of the compounds. The I_{pc}/I_{pa} ratio is close to unity in all the compounds investigated. However, this ratio is generally lower in the secondary amines in comparison with their corresponding Schiff bases. This could be as a result of the broken conjugation in the amines thus causing a somewhat pseudo reversible behaviour in compounds **9–14**. The electro-

chemical behaviour of the compounds studied here is consistent with that observed in similar ferrocenyl Schiff base compounds.[73]

3.7. Antimicrobial Studies

The antimicrobial studies were carried out *via* the disc diffusion method. In this method, the standardized microorganisms isolate were spread on an agar plate. Thereafter, paper discs containing specific concentration of test compound were placed on the seeded agar and incubated at 37 °C for 24 h (see Section 2.5.2). The susceptibility of microorganisms to the test compounds was observed as a zone of inhibition around the discs (i.e. the
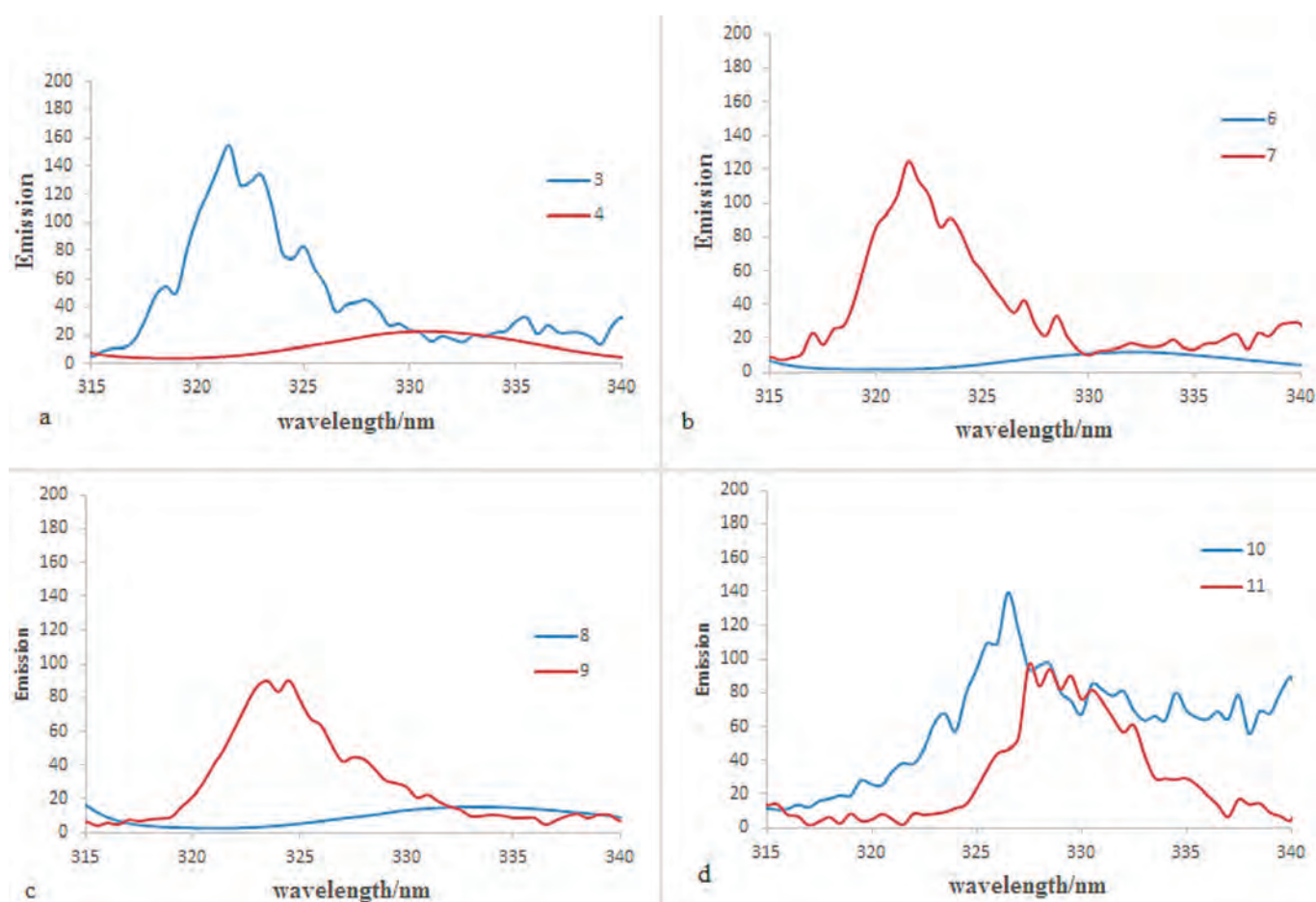
Figure 5 Emission spectra of compounds **3–4** (**a**), **6–7** (**b**), **8–9** (**c**) and **10–11** (**d**) determined in methanol.
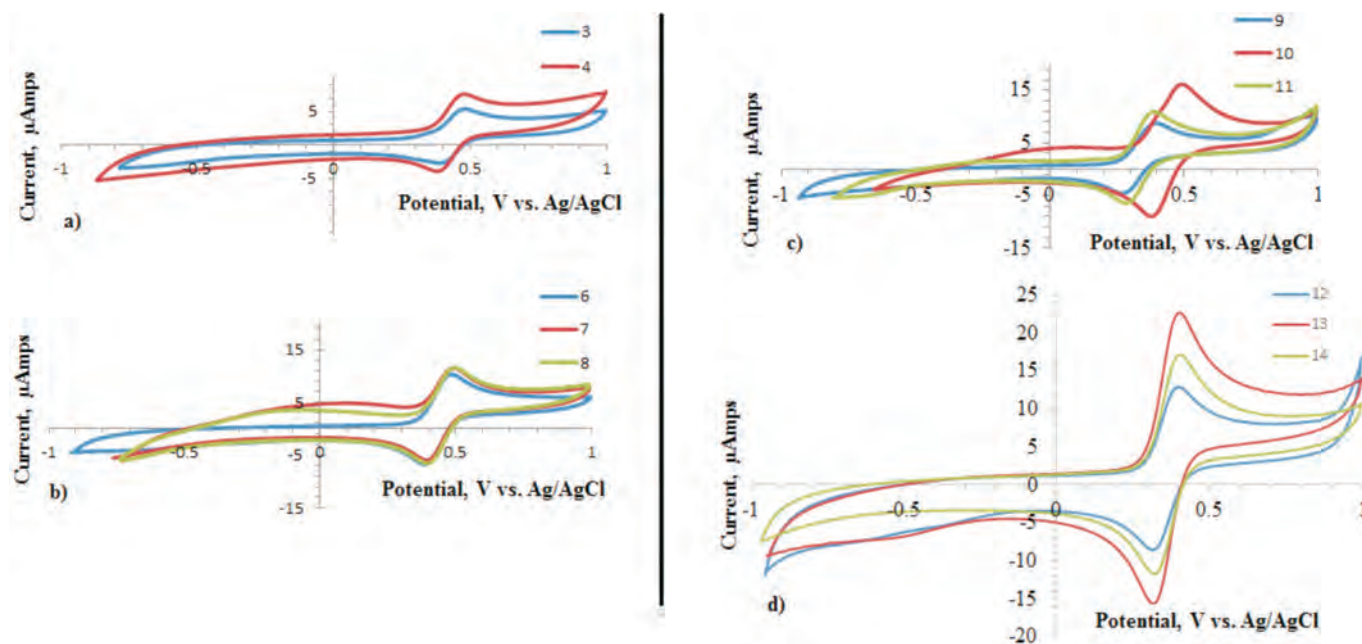
Figure 6 Cyclic voltammograms of (**a**) compounds **3** and **4**; (**b**) compounds **6–8**; (**c**) compounds **9–11** and (**d**) compounds **12–14** (*ca.* 2.0 × 10^{-4} M) in 0.1 M NaOCl/CH$_3$CN solution, initiated by the anodic sweep at a stationary Pt disk electrode, scanned at rate of 0.1 V s^{-1} against Ag/Ag$^+$ reference electrode at ambient temperature.

microorganism does not grow around the disc thus forming a clear region). After incubation time, antimicrobial activity was evaluated by measuring the zone of inhibition against the test organisms and compared with that of the standard. Antimicrobial activities were expressed as inhibition diameter zones in millimetres (mm). The experiment was carried out in triplicate, and the average zone of inhibition was calculated. This was done for the test compounds **3–14**, a negative control (DMSO) and positive controls (standard drugs). Fluconazole was used as the standard (positive control) for *Candida albicans*. This is because the fungus is highly susceptible the drug and thus is usually used as a positive control agent for the fungus.[80–82] Fluconazole has been used as a standard drug in numerous Chloramphenicol is a broad-spectrum antibiotic and is effective against several bacteria including the ones used in this study and has been employed as a standard in similar studies.[83–85] It was thus was selected as positive control agent for the bacteria species. The inhibition zones (i.e antimicrobial activity) of the test compounds **3–14** are reported in Table 9 as percentages relative to activity of the standard drugs used.

The antimicrobial properties of compounds **3–14** were individ-ually studied against the bacterial species *Escherichia coli, Salmonella typhimirium, Staphylococcus aureus* and fungal species *Candida albicans*. These were tested at a concentration of 20 *μ*g/0.02 mL in DMSO solution using a paper-disc diffusion method. The solutions of the compounds under investigation in DMSO were used immediately after preparation. The experiment was carried out in triplicate, and the average zone of inhibition was calculated. The results of these studies indicate the compounds have variable activities against the test organisms, as shown in Table 9. In general, the compounds were more active towards the Gram-positive bacteria *Staphylococcus aureus* and fungus *Candida albicans* and showed lesser inhibition against the Gram-negative bacteria *Escherichia coli* and *Salmonella typhimirium*. Compound **14** showed high activity against all test organisms, with inhibitions >60 %. Compound **10** also showed good inhibitions, >60 %, against the test organisms except *Escherichia coli* where it showed 45 % inhibition. The fungus *Candida albicans*, was susceptible to all the compounds except compound **13** which showed no activity. Nitrogen heterocyclic ferrocenyl Schiff bases studied elsewhere showed similar biological activity like the one observed here.[35] The information on the biological

Table 8 Cyclic voltammetry data of the compounds **3–6** and **8–14** (*ca.* 2.0 × 10^{-4} M) in acetonitrile , 0.1 M NaOCl, at a stationary platinum-disk electrode with internal diameter 0.3 cm and scanned at a rate of 0.1 V s^{-1} at 25 °C, potential scale referenced to Ag/Ag$^+$ electrode.

Compound	E_{pc} /V	E_{pa} /V	ΔE_P	E°/V	I_{pc} /µA	I_{pa} /µA	I_{pc}/I_{pa}	n
Ferrocene	0.4138	0.4703	0.0565	0.4421	30.736	26.2050	1.17	1.04
3	0.4582	0.4106	0.04761	0.4344	3.3588	3.1218	0.92	1.24
4	0.4642	0.3987	0.06546	0.4314	4.1822	4.9260	0.85	0.90
5	0.4047	0.4642	0.05951	0.4344	9.8192	8.5585	0.99	0.99
6	0.4761	0.4106	0.06546	0.4433	7.519	7.9625	0.94	0.90
8	0.4820	0.4106	0.07142	0.4463	9.3492	8.2820	1.13	0.83
9	0.3670	0.2916	0.07736	0.3303	5.1102	4.6078	1.10	0.76
10	0.4761	0.3987	0.07736	0.4374	11.124	10.9921	1.01	0.76
11	0.3690	0.3035	0.06546	0.3362	10.46	6.4620	1.20	0.90
12	0.3987	0.3214	0.07736	0.3600	10.9110	10.5252	1.04	0.76
13	0.4166	0.3214	0.09521	0.3690	22.8240	21.2390	1.07	0.62
14	0.4047	0.3214	0.08331	0.3630	17.159	14.0000	1.23	0.71

Table 9 Summary of antibacterial activities of compounds **3–14** in DMSO.

Compound	Microbial species			
	Escherichia coli	*Salmonella typhimirium*	*Staphylococcus aureus*	*Candida albicans*
3	+++	+	+++	++++
4	++	+	+++	+++
5	+	–	+	++
6	+	+	+++	+++
7	+++	+	+++	+++
8	+++	+	+++	++++
9	+	–	+	+++
10	+	–	+	++
11	+	–	+	++
12	++	++++	++++	++++
13	–	+	++	–
14	+++++	++++	++++	++++
FLUC	Not tested	Not tested	Not tested	++++++++
CM	+++++++	+++++++	++++++	Not tested
DMSO	–	–	–	–

Key: Inhibition zone diameter in mm (% inhibition): where '–' means no activity, '+' 6–7 mm (30–35 %), '++' 8–9 mm (40–45 %), '+++' 10–11 mm (50–55 %) '++++' 12–13 mm (60–65 %) and '+++++' 14–15 mm (70–75 %) inhibition. Percentage inhibition values are reported relative to inhibition zones of standard drugs chloramphenicol (CM) for bacteria and fluconazole (FLUC) for the fungus.

activity of ferrocene-containing Schiff base and amine compounds reported here warrants further investigation to ascertain their structure activity relationship. This could in turn help in the design of more similar compounds for biological applications. There are high prospects that this activity could be improved by complexation of biologically active metals with these ferrocenyl-*N*-(pyridinylmethylene)anilines or ferrocenyl-N-(pyridinylmethyl)anilines metalloligands. This will offer a new class of bimetallic medicinal compounds that will go a long way in sustaining the fight against infectious and non-infectious diseases.

4. Conclusion

Solvent-free grinding of ferrocenylaniline with a pyridinecarboxaldehyde yielded corresponding Schiff bases in excellent yields in a very short time. This reaction proceeded *via* the condensation reaction where water was eliminated. The mechanochemistry grinding technique was also successfully applied in reduction of the Schiff bases to their corresponding secondary amines by use of $NaBH_4$, activated on neutral Al_2O_3 support in solid phase. The desired amine products were obtained in excellent yields and also in very short time. Hence, this technique is cleaner, simpler, greener, timeous and pure products were achieved with minimum work-up. Characterization of the synthesized compounds was successfully performed using FT-IR, ¹H-NMR, ¹³C-NMR and X-ray crystallography techniques. All data obtained are consistent with the proposed structures. Heat flow curves for these compounds show single major event of melting followed by decomposition. The melting temperature from DSC technique corresponds with those obtained from melting point apparatus. From the detailed solvatochromic studies performed, the compounds show a blue shift (compared to ferrocene) in moving from polar to non-polar solvent albeit the shift being smaller in the amines. These compounds are thus good candidates for further investigation as sensors and in molecular electronics for construction of molecular switches. Also, the nonlinear optical susceptibilities and hyperpolarizability of these compounds should be investigated. Electrochemical traits of all the compounds were studied relative to that of ferrocene by cyclic voltammetry. In all the compounds, one electron redox behaviour was observed. The voltammograms showed one cathodic peak and a corresponding anodic peak occurring at the platinum electrode in the range 0.2916–0.4642 V. Electrochemical studies reveal that the electron withdrawing imine group substantially influences the redox potential of the iron centre of ferrocene moiety compared to amine group. Based on the variation observed in the formal potential values of compounds **3–14**, it can be concluded that the oxidation potential of the ferrocenyl oxidizing moiety, can be modified by changing the electronic properties of the substituents attached to the cyclopentadienyl ring *via* changing the imine to amine. Finally, these compounds show good inhibitory antimicrobial activity against fungus *Candida albicans* and Gram-positive bacterium *Staphylococcus aureus* and mild activity against Gram-negative bacteria *Escherichia coli* and *Salmonella typhimirium* in comparison with standard drugs. Improvement of the antimicrobial potency of the compounds reported here as well as other properties will be investigated further by coordination of selected transition metals to these metalloligands hence forming versatile multimetallic complexes. To this end, we are pursuing synthesis of potent antimicrobial and anticancer compounds as well as non-linear optical compounds by complexation of selected transition metals using these compounds. We anticipate that the bimetallic compounds obtained thereafter will be of high utility in varying fields.

Supplementary Material

CCDC 1435546–1435549 contains the supplementary crystallographic data for this paper. These data can be obtained free of charge from The Cambridge Crystallographic Data Centre *via* www.ccdc.cam.ac.uk/data_request/cif. Supplementary Fig. S1 to Fig. S14 in the online supplement show the IR spectra of compounds **1–14**, respectively; Fig. S15 to Fig. S26 show the ESI mass spectra of compounds **3–14**, respectively; Fig. S27 to Fig. S40 show the ¹H-NMR spectra of compounds **1–14**, respectively; and Fig. S41 to Fig. S54 show the ¹³C-NMR spectra of compounds **1–14**, respectively.

RESEARCH ARTICLE

E.M. Njogu, B. Omondi and V.O. Nyamori,
S. Afr. J. Chem., 2016, **69**, 51–66,
<http://journals.sabinet.co.za/sajchem/>.

65

References

1 T. Kealy and P. Pauson, A new type of organo-iron compound. *Nature*, 1951, **168**, 1039–1040.

2 S. A. Miller, J.A. Tebboth and J.F. Tremaine, Di cyclo pentadienyliron. *J. Chem. Soc.*, 1952, 632–635.

3 G. Wilkinson, M. Rosenblum, M. Whiting and R. Woodward, The structure of iron bis-cyclopentadienyl. *J. Am. Chem. Soc.*, 1952, **74**, 2125–2126.

4 P. F. Eiland and R. Pepinsky, X-ray examination of iron biscyclopentadienyl. *J. Am. Chem. Soc.*, 1952, **74**, 4971–4971.

5 J. Dunitz and L. Orgel, Bis-cyclopentadienyl iron: a molecular sandwich. *Nature*, 1953, **168**, 121–122.

6 H. Werner, At least 60 years of ferrocene: the discovery and rediscovery of the sandwich complexes. *Angew. Chem., Int. Ed.*, 2012, **51**, 6052–6058.

7 D. R. Van Staveren and N. Metzler-Nolte, Bioorganometallic chemistry of ferrocene. *Chem. Rev.*, 2004, **104**, 5931–5986.

8 A. Togni, Ferrocene-containing charge transfer complexes. Conducting and magnetic materials, in *Ferrocenes: Homogeneous Catalysis, Organic Synthesis, Materials Science*, (A. Togni and T. Hayashi, eds.), John Wiley & Sons, New York, 2008, pp. 433–469

9 Z. Akhter, A. Nigar, M.Y. Razzaq and H.M. Siddiqi, Synthesis and physico-analytical studies of some novel ferrocenyl Schiff base derivatives. *J. Organomet. Chem.*, 2007, **692**, 3542–3546.

10 T. Seshadri, Novel ferrocene-based chiral Schiff's base derivative with a twist-grain boundary phase (TGBA) and a blue phase. *Chem. Commun.*, 1998, 735–736.

11 S. Sakanishi, D.A. Bardwell, S. Couchman, J.C. Jeffery, J.A. McCleverty and M.D. Ward, Donor/acceptor complexes containing ferrocenyl-pyridine ligands attached to a tungsten carbonyl centre: Structural, spectroscopic and electrochemical properties. *J. Organomet. Chem.*, 1997, **528**, 35–45.

12 J.M. Casas-Solvas, E. Ortiz-Salmerón, I. Fernández, L. García-Fuentes, F. Santoyo-González and A. Vargas-Berenguel, Ferrocene–β-cyclodextrin conjugates: synthesis, supramolecular behavior, and use as electrochemical sensors. *Chem. – Eur. J.*, 2009, **15**, 8146–8162.

13 M.S. Driver and J.F. Hartwig, A second-generation catalyst for aryl halide amination: mixed secondary amines from aryl halides and primary amines catalyzed by (DPPF) PdCl$_2$. *J. Am. Chem. Soc.*, 1996, **118**, 7217–7218.

14 S.M. Bruno, A.C. Gomes, A.C. Coelho, P. Brandão, A.A. Valente, M. Pillinger and I.S. Gonçalves, Catalytic isomerisation of α-pinene oxide in the presence of ETS-10 supported ferrocenium ions. *J. Organomet. Chem.*, 2015, **791**, 66–71.

15 S. Siangwata, N. Baartzes, B.C. Makhubela and G.S. Smith, Synthesis, characterisation and reactivity of water-soluble ferrocenylimine-Rh(I) complexes as aqueous-biphasic hydroformylation catalyst precursors. *J. Organomet. Chem.*, 2015, **796**, 26–32.

16 C. Ornelas, Application of ferrocene and its derivatives in cancer research. *New J. Chem.*, 2011, **35**, 1973–1985.

17 W. Hegazy, Synthesis of organometallic-based biologically active compounds: in vitro antibacterial and antifungal of asymmetric ferrocene-derived Schiff-bases chelates. *Int. Res. J. Pure Appl. Chem.*, 2012, **2**, 170.

18 S. K. Verma and V.K. Singh, Synthesis and characterization of ferrocene functionalized transition metal dithiocarbamate complexes: Investigations of antimicrobial, electrochemical properties and a new polymorphic form of [Cu {κ^{2}S,S-S$_2$CN (CH$_2$C$_4$H$_3$O) CH$_2$Fc}$_2$]. *J. Organomet. Chem.*, 2015, **791**, 214–224.

19 M. José Calhorda, P.J. Costa, P.N. Martinho, M. Concepción Gimeno, A. Laguna, S. Quintal and M. Dolores Villacampa, Synthesis and ligand properties towards gold and silver of the ferrocenylamidobenzimidazole ligand. *J. Organomet. Chem.*, 2006, **691**, 4181–4188.

20 S. Quintal, M. Concepción Gimeno, A. Laguna and M.J. Calhorda, Silver (I) and copper (I) complexes with ferrocenyl ligands bearing imidazole or pyridyl substituents. *J. Organomet. Chem.*, 2010, **695**, 558–566.

21 J. Rajput, J.R. Moss, A.T. Hutton, D.T. Hendricks, C.E. Arendse and C. Imrie, Synthesis, characterization and cytotoxicity of some palladium (II), platinum (II), rhodium (I) and iridium (I) complexes of ferrocenylpyridine and related ligands. Crystal and molecular structure of trans-dichlorobis (3-ferrocenylpyridine) palladium (II). *J. Organomet. Chem.*, 2004 **689**, 1553–1568.

22 E.W. Neuse, Macromolecular ferrocene compounds as cancer drug models. *J. Inorg. Organomet. Polym. Mater.*, 2005, **15**, 3–31.

23 S. Yavuz and H. Yıldırım, Ferrocene derivatives carrying urea, thiourea, and sulfonamide moieties: synthesis and evaluation of antibacterial and antifungal activities. *J Chem.*, 2013, **2013**, 1–7.

24 C. Biot, N. François, L. Maciejewski, J. Brocard and D. Poulain, Synthesis and antifungal activity of a ferrocene-fluconazole analogue. *Bioorg. Med. Chem. Lett.*, 2000, **10**, 839–841.

25 I. S. Lee, S.S. Lee, Y.K. Chung, D. Kim and N.W. Song, Preparation and properties of ferrocenyl bimetallic compounds for non-linear optics. *Inorg. Chim. Acta*, 1998, **279**, 243–248.

26 J. Mata, S. Uriel, E. Peris, R. Llusar, S. Houbrechts and A. Persoons, Synthesis and characterization of new ferrocenyl heterobimetallic compounds with high NLO responses. *J. Organomet. Chem.*, 1998, **562**, 197–202.

27 B. Shafaatian, M. Hashemibagha, B. Notash and S.A. Rezvani, Synthesis, characterization, X-ray crystal structure, luminescence, electrochemical and solvatochromism studies of new dimer of nickel and palladium complexes containing ferrocenyl imine ligand. *J. Organomet. Chem.*, 2015, **791**, 51–57.

28 J. Rajput, A.T. Hutton, J.R. Moss, H. Su and C. Imrie, Ferrocenyl-nitrogen donor ligands. Synthesis and characterization of rhodium (I) complexes of ferrocenylpyridine and related ligands. *J. Organomet. Chem.*, 2006, **691**, 4573–4588.

29 C. Imrie, P. Engelbrecht, C. Loubser, C.W. McCleland, V.O. Nyamori, R. Bogardi, D.C. Levendis, N. Tolom, J. van Rooyen and N. Williams, Synthesis of ferrocenylphenyl derivatives including biphenylferrocenes, arylferrocenylphenyl ethers and arylferrocenylphenyl amines. *J. Organomet. Chem.*, 2002, **645**, 65–81.

30 C. J. Richards and A.W. Mulvaney, Synthesis of phosphinoferrocenyloxazolines. New ligands for asymmetric catalysis. *Tetrahedron: Asymmetry*, 1996, **7**, 1419–1430.

31 D. Braga, M. Polito, M. Bracaccini, D. D'Addario, E. Tagliavini, D.M. Proserpio and F. Grepioni, Novel hetero-bimetallic metalla-macrocycles based on the bis-1-pyridyl ferrocene [Fe (η^5-C$_5$H$_4$-1-C$_5$H$_4$N)$_2$] ligand. Design, synthesis and structural characterization of the complexes [Fe (η5-C$_5$H$_4$-1-C$_5$H$_4$N)$_2$](Ag^I)$_2$$^{2+}$/(Cu^{II})$_2$$^{4+}$/(Zn^{II})$_2$$^{4+}$. *Chem Commun.*, 2002, 1080–1081.

32 P. Stepnicka, *Ferrocenes: Ligands, Materials and Biomolecules*, John Wiley & Sons, 2008.

33 N. Lease, V. Vasilevski, M. Carreira, A. de Almeida, M. Sanaú, P. Hirva, A. Casini and M. Contel, potential anticancer heterometallic Fe–Au and Fe–Pd agents: initial mechanistic insights. *J. Med. Chem.*, 2013, **56**, 5806–5818.

34 P. Govender, H. Lemmerhirt, A.T. Hutton, B. Therrien, P.J. Bednarski and G.S. Smith, First- and second-generation heterometallic dendrimers containing ferrocenyl-ruthenium(ii)-arene motifs: synthesis, structure, electrochemistry, and preliminary cell proliferation studies. *Organometallics.*, 2014, **33**, 5535–5545.

35 Z.H. Chohan and M. Praveen, Synthesis, characterization and antibacterial properties of symmetric 1, 1'-ferrocene derived Schiff-base ligands and their Co (II), Cu (II), Ni (II) and Zn (II) chelates. *Appl. Organomet. Chem.*, 2000, **14**, 376–382.

36 Z.H. Chohan, M.F. Jaffery and C.T. Supuran, antibacterial Co (II), Cu (II), Ni (II) and Zn (II) complexes of thiadiazoles Schiff bases. *Met.-Based Drugs.*, 2001, **8**, 95.

37 S.M. Quan and P.L. Diaconescu, High activity of an indium alkoxide complex toward ring opening polymerization of cyclic esters. *Chem commun.*, 2015, **51**, 9643–9646.

38 T. Seshadri, H.J. Haupt, U. Flörke and G. Henkel, Novel cholesteric glassy liquid crystals of monosubstituted ferrocenes: synthesis and selective reflection properties of a dimesogen, and crystal structure of a monomesogen. *Liq. Cryst.*, 2007, **34**, 33–47.

39 R.M. Onofrei, I. Carlescu, G. Lisa, M. Silion, N. Hurduc and D. Scutaru, Synthesis and liquid crystalline behavior of some monosubstituted ferrocene containing schiff bases. *Rev. Chim.*, 2012, **63**, 139–145

40 G. Yaman, C. Kayran and S. Özkar, Pentacarbonyl (2-ferrocenyl-pyridine) metal (0) complexes of Group 6 elements. Synthesis and characterization. *Transition Met. Chem.*, 2005, **30**, 53–57.

41 K. Osakada, T. Sakano, M. Horie and Y. Suzaki, Functionalized ferrocenes: unique properties based on electronic communication

between amino group of the ligand and Fe center. *Coord. Chem. Rev.*, 2006, **250**, 1012–1022.

42 E.M. Barranco, O. Crespo, M.C. Gimeno, P.G. Jones and A. Laguna, M.D. Villacampa, Synthesis, structure and redox behaviour of gold and silver complexes with 3-ferrocenylpyridine. *J. Organomet. Chem.*, 1999, **592**, 258–264.

43 P. Barbaro, C. Bianchini, G. Giambastiani and S.L. Parisel, Progress in stereoselective catalysis by metal complexes with chiral ferrocenyl phosphines. *Coord. Chem. Rev.*, 2004, **248**, 2131–2150.

44 A. Fihri, P. Meunier and J.-C. Hierso, Performances of symmetrical achiral ferrocenylphosphine ligands in palladium-catalyzed cross-coupling reactions: a review of syntheses, catalytic applications and structural properties. *Coord. Chem. Rev.*, 2007, **251**, 2017–2055.

45 S.-J. Jo, Y.-E. Jin, J.-H. Kim and H.-S. Suh, Synthesis of ferrocenyl and diphenyl substituted bispyridino-18-crown-6 ether for chiral recognition. *Bull. Korean Chem. Soc.*, 2007, **28**, 2015–2019.

46 V.C. Gibson, N.J. Long, P.J. Oxford, A.J. White and D.J. Williams, Ferrocene-substituted bis (imino) pyridine iron and cobalt complexes: toward redox-active catalysts for the polymerization of ethylene. *Organometallics*, 2006, **25**, 1932–1939.

47 Z.H. Chohan, Antibacterial copper (II) complexes of 1, 1′-symmetric ferrocene-derived Schiff-base ligands: studies of the effect of anions on their antibacterial properties. *Appl. Organomet. Chem.*, 2002, **16**, 17–20.

48 S. Kathiravan, R. Raghunathan, G. Suresh and G.V. Siva, Synthesis and antimicrobial activities of novel ferrocenyl dispiropyrrolidines and pyrrolizidines. *Med. Chem. Res*, 2012, **21**, 3170–3176.

49 A. A. Abou-Hussein and W. Linert, Synthesis, spectroscopic, coordination and biological activities of some organometallic complexes derived from thio-Schiff base ligands. *Spectrochim. Acta, Part A*, 2014, **117**, 763–771.

50 T. Stringer, H. Guzgay, J.M. Combrinck, M. Hopper, D.T. Hendricks, P.J. Smith, K.M. Land, T.J. Egan and G.S. Smith, Synthesis, characterization and pharmacological evaluation of ferrocenyl azines and their rhodium (I) complexes. *J. Organomet. Chem.*, 2015, **788**, 1–8.

51 I.S. Lee, D.M. Shin and Y.K. Chung, Self-assembly of organometallic-organic hybrid supramolecular arrays from ferrocenyl dipyridines and aromatic carboxylic acids. *Cryst. Growth Des.*, 2003, **3**, 521–529.

52 W. Yu, J. Jia, J. Gao, L. Han and Y. Li, Synthesis, characterization and third-order nonlinear optical properties of symmetrical ferrocenyl Schiff base materials. *Chem. Phys. Lett.*, 2015, **624**, 47–52.

53 S. Fery-Forgues and B. Delavaux-Nicot, Ferrocene and ferrocenyl derivatives in luminescent systems. *J. Photochem. Photobiol., A*, 2000, **132**, 137–159.

54 E.M. Barranco, O. Crespo, M.C. Gimeno, P.G. Jones, A. Laguna and C. Sarroca, 1, 1′-Bis (2-pyridylthio) ferrocene: a new ligand in gold and silver chemistry. *J. Chem. Soc., Dalton Trans.*, 2001, 2523–2529.

55 E.M. Barranco, M.C. Gimeno, A. Laguna and M.D. Villacampa, Gold and silver complexes with the ferrocenyl-pyrazolate ligand FcCH₂pz. *Inorg. Chim. Acta*, 2005, **358**, 4177–4182.

56 W.M. Xue, F.E. Kühn, E. Herdtweck and Q. Li, Organometallic polymers with the backbone consisting of ferrocene and bimetallic tetracarboxylates. *Eur. J. Inorg. Chem.*, 2001, **2001**, 213–221.

57 N.C. Tice, S. Parkin and J.P. Selegue, Synthesis, characterization and crystal structures of boron-containing intermediates in the reductive amination of ferrocenecarboxaldehyde to a bis(ferrocenylmethyl) amine. *J. Organomet. Chem.*, 2007, **692**, 791–800.

58 M.V. Lokhande and M. Gulam Farooq, Spectral studies of some transition metal ion complexes with 4-[(E)-(ferrocene-1-methylidene) amino] pyridin-2-ol. *J. app. Chem.*, 2014, **6**, 36–42.

59 M. Gulam Farooq and M.V. Lokhande. Synthesis of ferrocene based organometallic compounds & antimicrobial activity. *J. app. Chem.*, 2014, **7**, 2278–5736

60 Y.-T. Liu, G.-D. Lian, D.-W. Yin and B.-J. Su, Synthesis, characterization and biological activity of ferrocene-based Schiff base ligands and their metal (II) complexes. *Spectrochim. Acta, Part A*, 2013, **100**, 131–137.

61 E.M. Cayuela, L. Xiao, T. Sturm, B.R. Manzano, F.A. Jalon and W. Weissensteiner, Synthesis of enantiopure 1, 1′-(1-dimethylamino-propanediyl) ferrocene *via* a highly diastereoselective imine reduction. *Tetrahedron: Asymmetry*, 2000, **11**, 861–869.

62 T. Lozano-Cruz, P. Ortega, B. Batanero, J.L. Copa-Patiño, J. Soliveri, F.J. de la Mata and R. Gómez, Synthesis, characterization and antibac-

63 P. Hu, K.-Q. Zhao and H.-B. Xu, 4-Nitrophenylferrocene. *Molecules*, 2001, **6**, M249.

64 S. Ali, A. Badshah, A.A. Ataf, B. Lal and K.M. Khan, Synthesis of 3-ferrocenylaniline: DNA interaction, antibacterial, and antifungal activity. *Med. Chem. Res*, 2013, **22**, 3154–3159.

65 V.O. Nyamori, G. Keru and B. Omondi, (4-{[(Pyridin-4-yl) methyli-dene] amino} phenyl) ferrocene. *Acta Crystallogr.*, 2012, **68**, m1535–m1535.

66 T. H. Tabane and G.S. Singh, A simple reduction of imines to biologically important secondary amines using sodium borohydride/alumina in solid-phase. *Proc. Natl. Acad. Sci., India, Sect. A*, 2014, **84**, 517–521.

67 Bruker, APEXII, Bruker AXS Inc, Madison, Wisconsin, USA, 2009.

68 G.M. Sheldrick, *Acta Crystallog. Sect. A*, 2008, A64, 112–122.

69 L.J. Farrugia, WinGX and ORTEP for Windows: an update, *Appl. Crystallogr.*, 2012, **45**, 849–854.

70 R. Arancibia, A.H. Klahn, G.E. Buono-Core, D. Contreras, G. Barriga, C. Olea-Azar, M. Lapier, J.D. Maya, A. Ibañez and M.T. Garland, Organometallic Schiff bases derived from 5-nitrothiophene and 5-nitrofurane: synthesis, crystallographic, electrochemical, ESR and antiTrypanosoma cruzi studies. *J. Organomet. Chem.*, 2013, **743**, 49–54.

71 V. Kovač, A. Višnjevac, V. Rapić and B. Kojić-Prodić, Ferrocene compounds. XL. synthesis and characterization of ferrocene Schiff bases. *J. Mol. Struct.*, 2004, **687**, 107–110.

72 F. Ossola, P. Tomasin, F. Benetollo, E. Foresti and P. Vigato, Synthesis, structure and properties of new ferrocene-containing compounds. *Inorg. Chim. Acta*, 2003, **353**, 292–300.

73 B.-X. Ye, Y. Xu, F. Wang, Y. Fu and M.-P. Song, Synthesis, structures and electrochemistry of two Schiff base compounds bearing phenylferrocene. *Inorg. Chem. Commun.*, 2005, **8**, 44–47.

74 C. Imrie, V.O. Nyamori and T.I. Gerber, Solvent-free synthesis of ferrocenylimines. *J. Organomet. Chem.*, 2004, **689**, 1617–1622.

75 C. Imrie, P. Kleyi, V.O. Nyamori, T.I. Gerber, D.C. Levendis and J. Look, Further solvent-free reactions of ferrocenylaldehydes: Synthesis of 1, 1′-ferrocenyldiimines and ferrocenylacrylonitriles. *J. Organomet. Chem.*, 2007, **692**, 3443–3453

76 Y. Yamaguchi, W. Ding, C.T. Sanderson, M.L. Borden, M.J. Morgan and C. Kutal, Electronic structure, spectroscopy, and photochemistry of group 8 metallocenes. *Coord. Chem. Rev.*, 2007, **251**, 515–524.

77 A. Acosta, J.I. Zink and J. Cheon, Ligand to ligand charge transfer in (hydrotris (pyrazolyl) borato)(triphenylarsine) copper(I). *Inorg. Chem.*, 2000, **39**, 427–432.

78 A.M. Asiri, Organometallic dyes: part 1. synthesis of orange to cyan dyes based on donor-conjugated-acceptor chromogens using ferrocene as the donor group. *Appl. Organometal. Chem.*, 2001, **15**, 907–915.

79 B. Delavaux-Nicot, J. Maynadié, D. Lavabre and S. Fery-Forgues, Ferrocenyl compound as a multiresponsive calcium chemosensor with remarkable fluorescence properties in CH₃CN. *Inorg. Chem.*, 2006, **45**, 5691–5702

80 M.S. Karthikeyan, B.S. Holla and N.S. Kumari, Synthesis and antimicrobial studies on novel chloro-fluorine containing hydroxy pyrazolines, *Eur. J. Med. Chem.*, 2007, **42**, 30–36.

81 P. Keyvan, B. Leila, R. Zahra, S. Manuchehr and Z. Kamiar, In vitro activity of six antifungal drugs against clinically important dermatophytes. *Jundishapur J. Microbiol.*, 2009, **4**, 158–163.

82 K. Zomorodian, M.J. Rahimi, K. Pakshir, M. Motamedi, M.R. Ghiasi and H. Rezashah, Determination of antifungal susceptibility patterns among the clinical isolates of *Candida* species. *J Global Infect. Dis.*, 2011, **3**, 357–360.

83 J. Vora, S. Vasava, K. Parmar, S. Chauhan and S. Sharma, Synthesis, spectral and microbial studies of some novel Schiff base derivatives of 4-methylpyridin-2-amine. *E-J. Chem.*, 2009 **6**, 1205–1210.

84 N.R. Bhalodia and V. Shukla, Antibacterial and antifungal activities from leaf extracts of *Cassia fistula* l.: an ethnomedicinal plant. *J. Adv. Pharm. Technol. Res.*, 2011, **2**, 104–109.

85 B. Chakraborty, U.K. Bhattacharyya and S. Nandy, Study of antimicrobial activity of methanolic extract of *Alangium lamarkii* leaves against selected microbial species. *Int. J. Pharm. Life Sci.*, 2012, **3**, 1620–1623.